



Machine learning approaches to predict the strength of graphene nanoplatelets concrete: Optimization and hyper tuning with graphical user interface



Turki S. Alahmari ^{a,*}, Kiran Arif ^{b,c,**}

^a Department of Civil Engineering, Faculty of Engineering, University of Tabuk, P.O. Box 741, Tabuk 71491, Saudi Arabia

^b Department of Computer Science, COMSATS University Islamabad, Wah Campus, 47040, Pakistan

^c Western Caspian University, Baku, Azerbaijan

ARTICLE INFO

Keywords:

Machine learning models
Shapley analysis
Graphical user interface
Compressive strength

ABSTRACT

This paper focuses on the need to consider the use of multipurpose cement composite (CC) in the construction industry to give superior performance. Therefore, incorporating nanomaterials (NMs) can improve the performance and characteristics of CC. Hence, the use of graphene nanoplatelets (GNPs) in the composite matrix can be a viable way to address the challenges towards achieving a sustainable, with superior properties. In addition, forecasting the properties of NMs is a challenging task due to nature of ambiguity between parameters, complex nature, and non-linear response to strength. In addition, strength evaluation is time consuming process. Thus, there is a needs for predictive models to estimate strength of NMs. This study employe four machine learning (ML) approaches namely as light gradient boosting (LGB), artificial neural network (ANN), gradient boosting (GB), and k-nearest neighbor (KNN) with hyper-tuning, and optimization. In addition, model evaluation is judge by statistical measures, uncertainty analysis, and tenfold approach is applied for validation of the model. Moreover, graphical user interface (GUI) is developed for practical implementation to estimate strength. The result reveals that XGB, and ANN model shows robust analysis with greater $R^2 > 0.90$ for both train and test sets with XGB perform better as compared to ANN and other models. XGB depicts lesser statistical index, and uncertainty analysis demonstrates all model with less level of ambiguity for train and test set. The train and test set for XGB, LGB, KNN, and ANN models demonstrate 7.668 %, 8.9 %, 8.9 %, 17.18 %, 9.85 %, 20.61, and 5 %, 14.74 %, respectively. Shapley analysis reveals that GNP thickness, diameter and curing have major contribution to strength.

1. Introduction

Concrete is utilized in the construction industry as one of the most prominent and well-known building materials in the world [1–3]. Consequently, it is imperative to acknowledge that the environmental consequences of the manufacturing process of concrete are detrimental

[4–6]. The production of concrete, which is primarily composed of Portland cement (PC), results in the consumption of nonrenewable materials such as sand, gravel, and freshwater, as well as the emission of carbon dioxide (CO_2) [7–10]. Subsequently, the environment is adversely affected due to malignant effects. The global estimated annual depletion of cement is 4 billion tons, with each ton of cement emitting an

Abbreviations: CC, cement composite; PC, portland cement; CO_2 , carbon dioxide; NPs, nanoparticles; NMs, nanomaterials; GNPs, graphene nanoplatelets; CM, cementitious matrix; ITZ, intersectional zone; C_3A , tri-calcium aluminate; MWCNTs, multi-walled carbon nanotubes; CNTs, carbon nanotubes; NS, nano silica; LWC, lightweight concrete; SF, silica fume; FA, fly ash; Al_2O_3 , aluminum oxide; SiO_2 , silica oxide; Fe_2O_3 , ferric oxide; AI, artificial intelligence; ML, machine learning; FS, flexural strength; CS, compressive strength; GEP, gene expression programming; SVM, support vector machine; MLPNN, multilayer perceptron neural network; DT, decision tree; GBT, gradient-boosted trees; KNN, k-nearest neighbors; SCMs, supplementary cementitious materials; ANN, artificial neural network; HPC, high-performance concrete; GUI, graphical User Interface; GB, gradient boosting; OF, objective function; RMSE, root mean square error; MAE, Mean Absolute Error; R^2 , coefficient of determination.

* Corresponding author.

** Corresponding author at: Department of Computer Science, COMSATS University Islamabad, Wah Campus, 47040, Pakistan.

E-mail addresses: talahmari@ut.edu.sa (T.S. Alahmari), kiranarif12345@gmail.com (K. Arif).

<https://doi.org/10.1016/j.mtcomm.2024.109946>

Received 2 May 2024; Received in revised form 13 July 2024; Accepted 24 July 2024

Available online 25 July 2024

2352-4928/© 2024 Elsevier Ltd. All rights are reserved, including those for text and data mining, AI training, and similar technologies.

Improved Mechanical Properties	Enhances compressive, tensile, and flexural strength due to better particle packing and cement hydration.
Durability	Increases resistance to environmental factors such as freeze-thaw cycles, chloride penetration, and sulfate attack.
Reduced Permeability	Decreases water and gas permeability, leading to enhanced durability and longevity.
Enhanced Workability	Improves the flow and placement of concrete mixtures without compromising strength.
Accelerated Hydration	Promotes early strength gain by accelerating the hydration process.
Crack Resistance	Minimizes crack formation and propagation due to improved toughness and ductility.
Self-Sensing Properties	Enables monitoring of structural health through changes in electrical resistance.
Self-Cleaning and Self-Healing	Contributes to self-cleaning surfaces and self-healing of micro-cracks through photocatalytic and chemical properties.
Eco-Friendly	Potential to reduce the overall carbon footprint by lowering cement content while maintaining performance.

Fig. 1. Nanomaterials significance in cementitious composite.

Table 1
Nanomaterials used in civil engineering.

Material	Nanomaterials	Abbreviations	Outcome effects	References
Cementitious composite	Carbon Nanotube	CNT	Strength and durability improvement	[64]
	Silicon dioxide	SiO ₂		[65]
	Titanium dioxide	TiO ₂	Strength and durability improvement with rapid hydration	[66]
	Chromium oxide	Cr ₂ O ₃	Mechanical strength enhancement	[67]
	Zinc dioxide	ZnO ₂		[68]
	Zirconium oxide	ZrO ₂		[69]
	Aluminum oxide	Al ₂ O ₃		[70]
	Calcium carbonate	CaCO ₃		[71]

equivalent amount of CO₂ [11]. PC is a finite resource that necessitates a substantial quantity of energy and is deliberated a vital constituent of cementitious matrix. Concrete, a cementitious composite is considered one of the main sources of CO₂ in the atmosphere. Thus, approximately considered for about seven percent of CO₂ emissions around the entire globe [12]. Additionally, its demand is increasing as a result of the advancements in modern construction projects such as dams, long bridges, etc [13,14]. In addition, concrete is characterized by a low strain capacity and a relatively low strength at initial load. However, there exists porous media inside the matrix, and increasing the load causes cracks [15]. Therefore, the mechanical aspect of the composite matrix is significantly diminished leading to reduced strength. Consequently, their inclusion in the composite medium enhances the strength and provides an adamant hindrance to cracking [16].

The exceptional performance of nanotechnology in various domains has garnered global interest [17–20]. Nanoparticles (NPs) are characterized by dimensions ranging from 1 to 100 nm. Nanomaterials (NMs) boost the strength and longevity of the material, while also improving hydration processes and reducing pressure on formwork [21–23]. Nanomaterials catalyze the formation of nucleation, resulting in the production of compact and less permeable CSH-hydrated products. Furthermore, the process of hydration involves a chemical reaction between NPs and calcium hydroxide, known as the pozzolanic reaction. This reaction leads to the expansion of CSH hydration products that leads to fills of the available voids due to dense structure [24–27]. A structure with reduced porosity and increased density is formed,

resulting in enhanced mechanical strength and durability [28–30]. Moreover, the small size of the concrete reinforcing material enhances its effectiveness in impeding fracture growth. Thus, reinforcement nanoparticles such as Graphene nanoplatelets (GNPs) and nanomaterials in cementitious composites have received significant attention for this reason. GNPs have attracted significant attention because of the distinct features associated with their tiny structure [31–33].

1.1. Literature review

A wide range of nanoparticles has been incorporated in cementitious matrix (CM) since the advent of nanotechnology. Nanomaterials have the strength and ability to enhance the resilience and efficacy with durability of concrete [34–36]. The addition of NPs to composite medium is primarily intended to enhance the microstructure of the cementitious component. Furthermore, the utilization of nanotechnology has garnered substantial interest in recent years, as depicted in Fig. 1.

Nanoparticles enhance the bulk characteristics of concrete by optimizing the packing model structure. Ultra or Nanoparticles can enhance the filler effect by improving the intersectional zone (ITZ) in cement and increasing the density of concrete [37–39]. Their manipulation or alteration in the cement matrix system occurs to create a new nanoscale structure by serving as an effective filler. NMs transform as they shoulder the role of novel binding agents that are smaller in size compared to cement particles [40,41]. This enhances the configuration

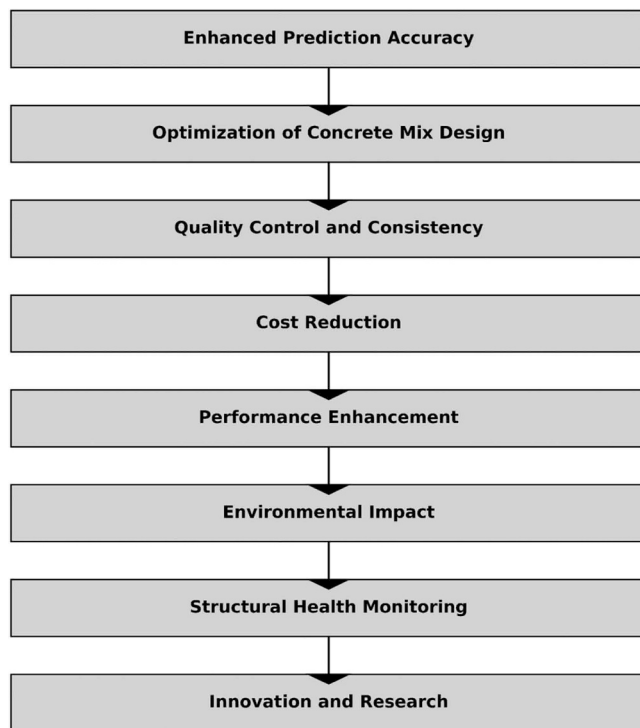


Fig. 2. Advantages of ML in concrete.

of the hydration gel, resulting in a tidy and cohesive hydration framework [42–44]. Furthermore, researchers have successfully created a novel type of concrete known as Nano concrete due to incorporation of NPs that act as fillers and additional chemical reactions inside the hydration system [45–51]. This innovative material exhibits improved durability and enhanced performance. In addition, the advancement of nanotechnology has generated significant research interest in the use of nano-materials in concrete over the past few decades [52–54]. Yang et al. [55] reported that the addition of nano-CaCO₃ to concrete significantly enhanced its compressive strength, impermeability, and resistance to carbonization after curing and de-moulding. The presence of nano-CaCO₃ in the cement hydration process resulted in its reaction with tri-calcium aluminate (C₃A), leading to the formation of hydrated calcium carbon aluminate. Shiho et al. [56] examined the microstructural characteristics of concrete samples containing NPs by conducting chloride diffusion tests and employing conventional scanning electron microscopy (SEM) methods. The SEM analysis demonstrates that the presence of NPs leads to a denser matrix, which in turn hinders the propagation of cracks. In addition, utilizing these NPs can enhance the performance and durability of concrete infrastructures [57]. Meng et al. [58] demonstrated that the characteristics of cement paste were significantly affected by the diameters of the particles. The author reveals that the NPs have a significant effect on the overall cementitious composite as reducing the size of NPs results in a denser and packed structure. Moreover, increasing size leads to strength enhanced as compared to control specimens. Ramezani et al. [59] discovered that multi-walled

carbon nanotubes (MWCNTs) had a higher level of compressive strength compared to flexural strength. In addition, Narasimman et al. [60] studied the effect of carbon nanotubes (CNTs), and nano-silica (NS) on the compressive strength of lightweight concrete (LWC). The author revealed that the incorporation of these nanofillers leads to a drastic increase in strength. Gunasekara et al. [61] investigated the influence of NS on the compressive strength of blended concrete. The author reveals that the addition of NS acts as a filler and increases the overall strength of the matrix. Sedaghatdoost et al. [29] assessed the flexural strengths of PC mortars by including MWCNTs at various concentrations ranging from 0 % to 0.15 %. The result shows that all configurations using CNTs exhibited greater flexural strengths after 28 days. Nili et al. [62] examined the effect of NS and silica fume (SF) on concrete and cement paste strength. The author used various concentration of both NPs and depicted that increasing their ranges, particularly the inclusion of 3 % or 5 % by weight of binder enhances the strength of both cementitious composites. Moreover, Oltulu et al. [63] investigated the impact of NPs on the compressive strength of cement mortar having fly ash (FA). The author utilized three NPs namely aluminum oxide (Al₂O₃), silica oxide (SiO₂), and ferric oxide (Fe₂O₃), and showed that their intrusion in the matrix enhances the overall strength of the composite. In addition, the overall effect of NPs on the cement matrix is depicted in Table 1.

1.2. Necessity of machine learning in civil engineering

Concrete is widely used worldwide as a construction material due to its notable advantages, such as cost-effectiveness, consistency, versatility, and durability [72–75]. Moreover, evaluating the mechanical characteristics of concrete is crucial for determining effective design strategies and the durability of structures against external forces. Also, the timely availability of experimental test findings is essential for the goal of minimizing costs and saving time [76–78]. To carry out studies, whether on-site or in a laboratory, advanced equipment must be used. As a result, a significant amount of work is required, making it economically impractical [79]. In addition, it is also vital and essential to have a specific area allocated for the storage and curing of concrete samples during testing. Therefore, leading to a rise in its financial ramifications. Furthermore, a substantial amount of time is required to perform a thorough analysis of the impact of certain components of concrete, such

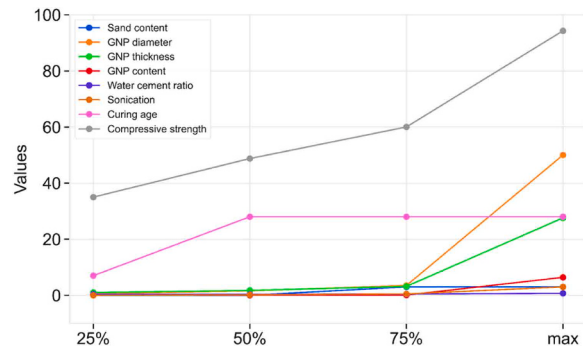


Fig. 3. Percentile graph of the dataset.

Table 2
Parameter descriptive statistics.

	Count	Mean	Standard deviation	Minimum	25 %	50 %	75 %	Maximum
Sand content	172	1.377	1.499	0.00	0.00	0.00	3.00	3.00
GNP diameter	172	3.38	6.87	0.072	0.55	1.60	3.5	50
GNP thickness	172	3.39	5.19	0.70	1.00	1.75	3.175	27.60
GNP content	172	0.26	0.94	0.010	0.025	0.04	0.08	6.40
Water cement ratio	172	0.40	0.10	0.20	0.33	0.37	0.45	0.72
Sonication	172	0.49	0.82	0.00	0.00	0.17	0.50	3.00
Curing age	172	19.7	10.8	1.00	7.00	28.0	28.0	28.0

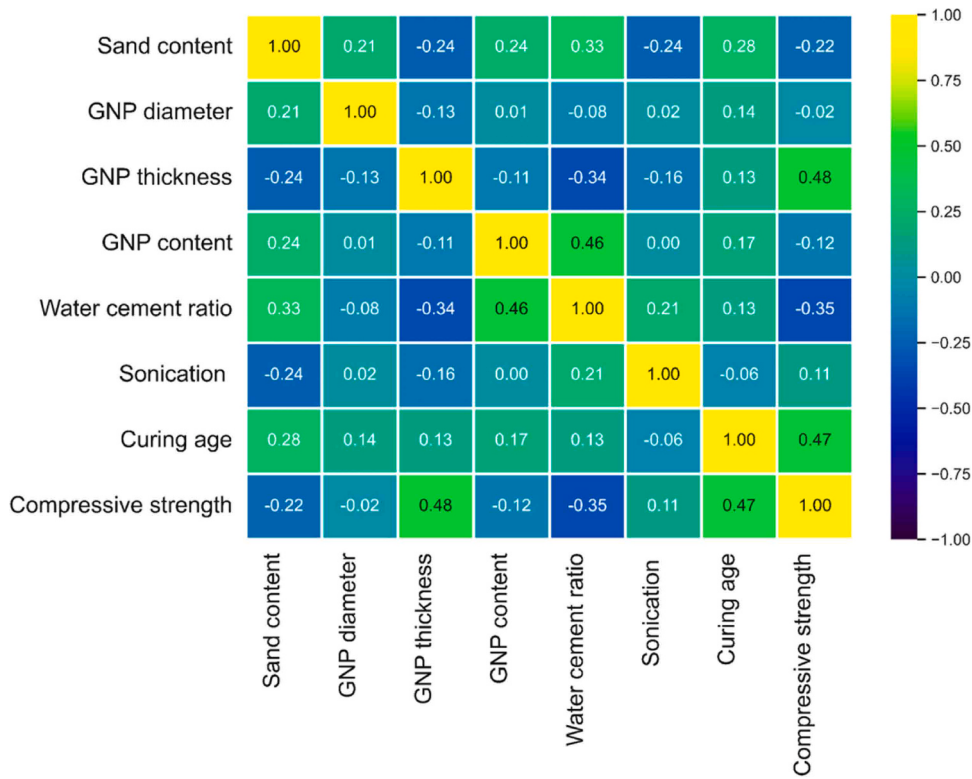


Fig. 4. Heat map of parameters to compressive strength.

as the composition of the mixture, the materials used for aggregates, and the duration of the curing process, on the compressive strength (CS) property of the matrix [80]. Thus, the distribution of these elements within the concrete mixture is random [81–83]. Evaluating the capability of concrete to endure compressive forces within a composite framework is a more demanding task. Therefore, precisely predicting the longevity of the concrete in a composite matrix is a challenging endeavor. To cater to these limitations, researchers suggested various correlations to assess the CS of the composite matrix in different laboratory conditions. These relations are predominantly established to calculate the CS of the cementitious matrix. Therefore, relying on this approach is impractical when handling different types of components in concrete. Consequently, this results in a reduction in the accuracy of estimation. The introduction of artificial intelligence (AI) and its application in the field of civil engineering can assist researchers in addressing many complex problems in the composite matrix. Unlike previous regression techniques, machine learning (ML) yields exceptionally precise outcomes [84–86].

ML approaches have a significant effect on the concrete mechanical properties, like CS, durability, and flexural strength (FS). Asif et al. [78] forecast the CS, and FS of plastic concrete by employing various approaches. The author used gene expression programming (GEP), support vector machine (SVM), multilayer perceptron neural network (MLPNN), decision tree (DT), and ensemble approaches, and reveals that the ensemble approach on SVM depicts robust performance. Nashat et al. [87] utilized nine different ML approaches including an ensemble, and revealed that gradient-boosted trees (GBT) give a strong correlation by showing greater R^2 and fewer errors. Mahdi et al. [88] employ five distant approaches including DT, SVM, k-nearest neighbors (KNN), random forest (RF), and artificial neural network (ANN) to predict CS of supplementary cementitious materials (SCMs). The author demonstrated that DT shows good performance with $R^2=0.96$ as compared to other models. Jiao et al. [89] predicted the CS of the concrete composite containing CNTs as nanomaterials with different algorithms including ensemble methods. The author concluded that the AdaBoost ensemble

approach gives the best performance. Zhang et al. [90] employed ML algorithms like SVM, KNN, and ANN for forecasting the chloride diffusion of concrete. The author reported that the SVM model shows greater accuracy as compared to other approaches. Furqan et al. [91] utilized various approaches with bagging and boosting to forecast the CS of high-performance concrete (HPC), and reported that bagging approaches with DT, and RF depict significant and robust correlation. In addition, the importance of machine learning in civil industry is depicted in Fig. 2.

1.3. Research significance

The objective of this study is to forecast the durability of concrete by integrating Graphene Nanoplatelets (GNPs). This is accomplished by utilizing a precompiled database derived from published publications. Therefore, the Extreme gradient boosting (XGB) technique, Light gradient boosting machines (LGB), and K-nearest neighbor (KNN) will be used to create these prediction models using anaconda spyder jupyter notebook. The efficacy of individual models is evaluated by using statistical matrices, and uncertainty analysis. In addition, feature importance is performed to determine the influential parameters in forecasting strength. Furthermore, a graphical User Interface (GUI) is developed using Python coding to determine the strength of nanocomposites in practical work.

2. Methodology

MLA is a computer-based algorithm that is useful in cementitious composite matrix for the prediction of properties [92–97]. Hence, regression and classification-based problems can be easily solved to achieve the desired results. Such methods are more prevalent in the concrete industry because ML approaches can analyze the behavior of materials from the training set, and make accurate forecasts from the test set [98–102]. Thus, based on the behavior of MLA, four methods are used including, XGB, LGB, KNN, and ANN for estimating the composite

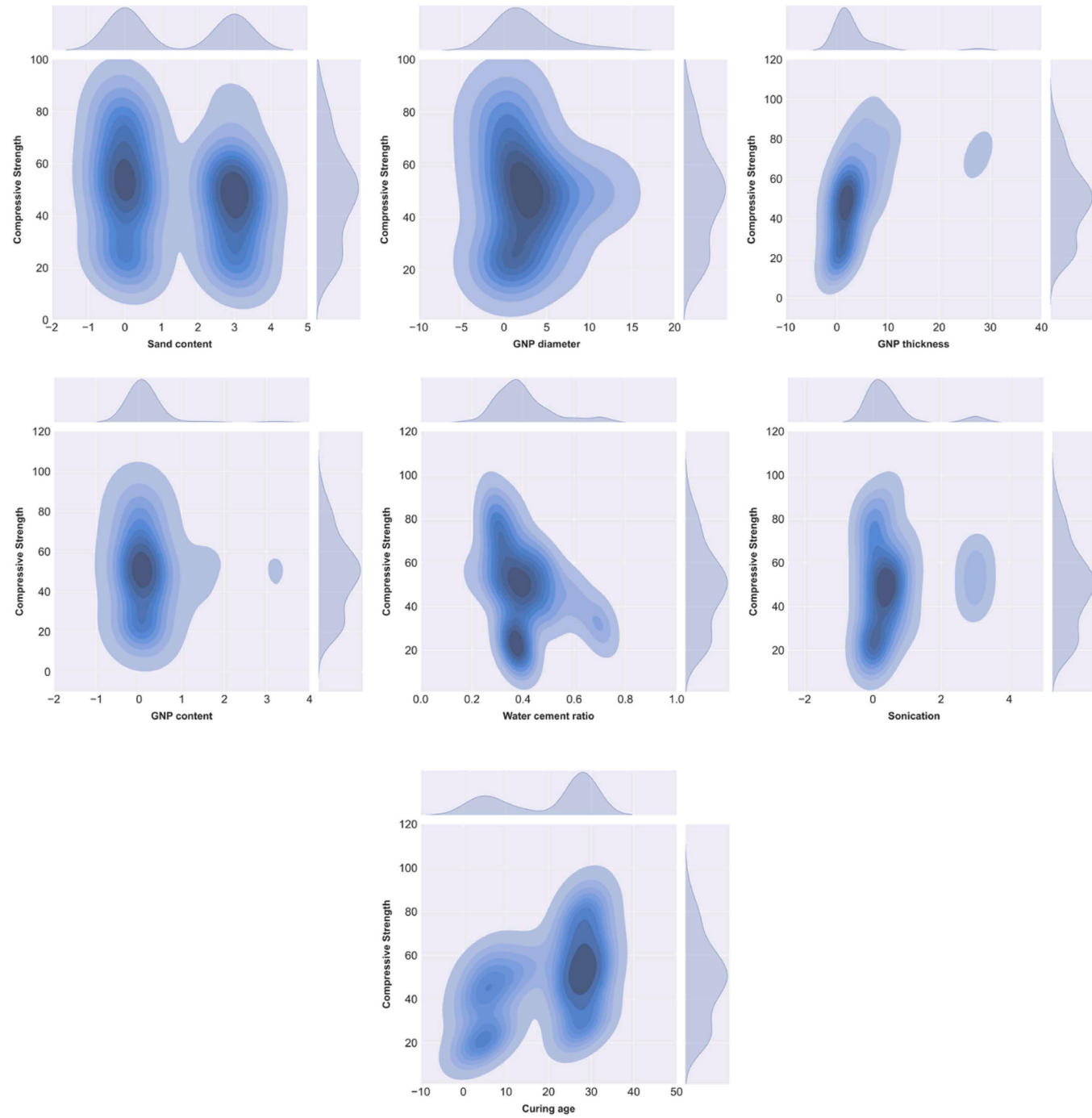


Fig. 5. Contour graphs of parameters.

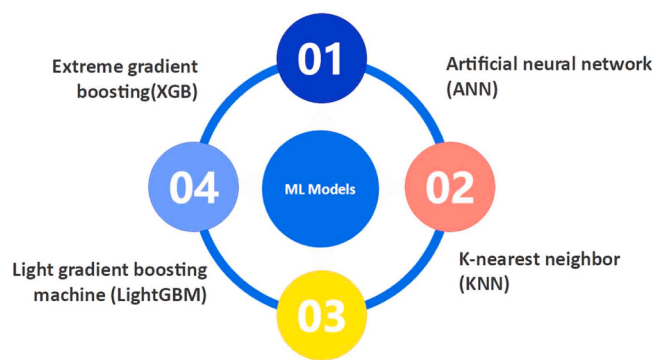


Fig. 6. ML approaches used in current research work.

strength containing nanoparticles. Moreover, the criteria for choosing these prominent approaches are based on their extraordinary predictive accuracy, model-complex nature, and robustness to overfitting. This makes them ideal for forecasting the strength of the matrix [103–107].

2.1. Data description

A complete database comprising 172 experimental data points of composite matrix incorporating GNPs has been compiled from earlier investigations. This database is used to assess the CS, as shown in **Annexure A**. Additionally, the description of data is essential in machine learning algorithms since it facilitates a comprehensive comprehension of the dataset's organization and the variables involved. Therefore, it is crucial to choose suitable algorithms. The dataset consists of 172 entries, comprising raw materials that are defined by their sand content, GNP diameter, thickness, and GNP content. In addition, the dataset also includes information on the GNP dispersion process, which involves the use of ultra-sonication, as well as the curing age. The dependent variable is the compressive strength of GNP. Thoroughly explaining these variables aids in recognizing pertinent characteristics and comprehending the connections among them, resulting in more precise and efficient construction of models. The correlation between the strength and the stated parameters was examined using Python metrics. Moreover, the command "VAC.describe(). T" is utilized to construct descriptive statistics that offer a concise overview of the mean, variability, and distribution pattern of a dataset. The command



Fig. 7. Flowchart of ML with details.

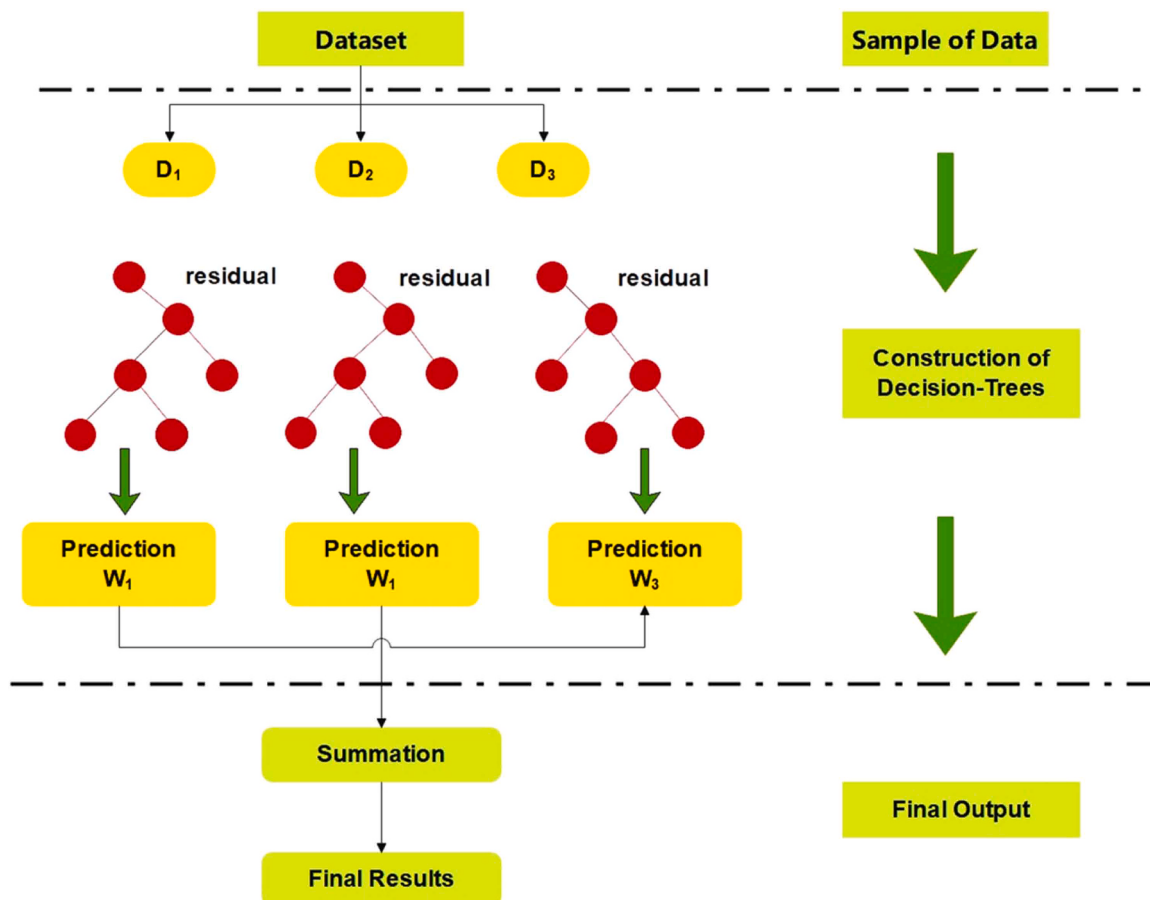


Fig. 8. Extreme gradient boosting prediction process.

calculates statistical measures of the entire dataset, including standard deviation, minimum, count, mean, maximum, and percentiles (25th, 50th, 75th) as depicted in [Table 2](#). The "percentiles" of the data frame offer a specific perspective on the 25th, 50th (median), and 75th percentiles and the maximum values for each variable in your dataset. The percentiles provide valuable insights into the distribution of each variable. Thus, allowing for the identification of the central tendency and the spread of the data points, as depicted in [Fig. 3](#).

[Fig. 4](#) displays the correlation heat map between CS and the input components. A negative correlation implies that as the amount of sand increases, the compressive strength generally decreases. Nevertheless, the association between sand content and compressive strength is feeble, indicating that sand content does not exert a significant influence on compressive strength. This phenomenon may be attributed to the possibility that an increased sand content could potentially weaken the binding characteristics of the cement, resulting in a less robust composite material. A moderate positive correlation indicates that there is a direct relationship between the increase in GNP thickness and the rise in compressive strength. Increasing the thickness of GNPs could enhance their ability to reinforce the material and enhance its structural integrity. Thus, resulting in greater strength. The presence of a weak negative association indicates that an increase in GNP content has a slight detrimental effect on compressive strength. This may occur due to an abundance of GNPs, which can result in the clumping together or inadequate spread of the particles inside the matrix. Hence, adversely impacting the mechanical characteristics of the material. Furthermore, the utilization of ultra-sonication can facilitate the uniform dispersion of GNPs throughout the matrix, hence raising the material's homogeneity and marginally augmenting its strength. A moderate positive correlation suggests that there is a connection between longer curing durations and

better compressive strength. During the curing process, the material undergoes hydration, which results in the gradual development of a more robust and long-lasting matrix.

[Fig. 5](#) illustrates the distribution of the input parameters and their associated output parameter for the use of the optimized benchmark system. These contour graphs illustrate the relationship between the individual range of the input parameters to the output strength of the concrete. The darkish regions indicate the specific density of each parameter related to concrete strength, as calculated from the data.

2.2. Machine learning overview

Machine learning is commonly used to predict the behavior of materials and other properties in the concrete matrix [\[108,109\]](#). The strength of a nanocomposite (GNPs) is predicted by using four algorithms namely XGB, LGB, KNN, and ANN. These techniques are well acknowledged for their outstanding performance and ability to precisely identify the attributes of properties [\[110–112\]](#). Furthermore, [Fig. 6](#) depicts the ML approaches employed in our research, while [Fig. 7](#) provides a detailed flowchart of MLA employed and input parameters. Furthermore, XGB, KNN, LGB, and ANN possess unique benefits when it comes to managing difficult datasets and collecting complex patterns. XGB and LGB were selected due to their outstanding performance in handling big datasets with high-dimensional features, their capacity to address overfitting, and their efficiency in managing missing data [\[113–115\]](#). KNN was chosen for its simplicity and robustness in analyzing local data structures, making it a useful benchmark for comparison [\[116–118\]](#). ANN was chosen for its robust ability to simulate non-linear connections and capture intricate patterns. By utilizing this varied range of models, our objective was to exploit their unique

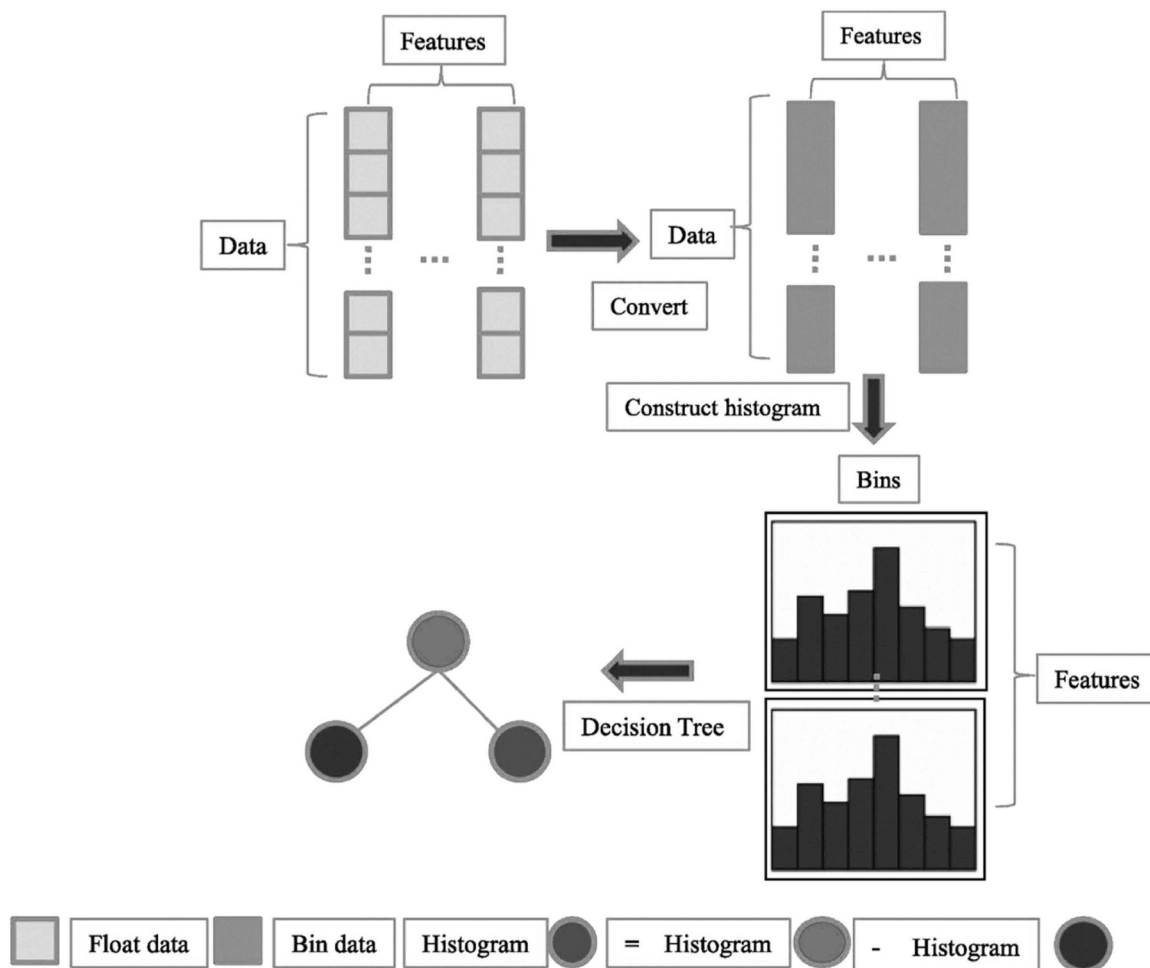


Fig. 9. Histogram-based decision tree.

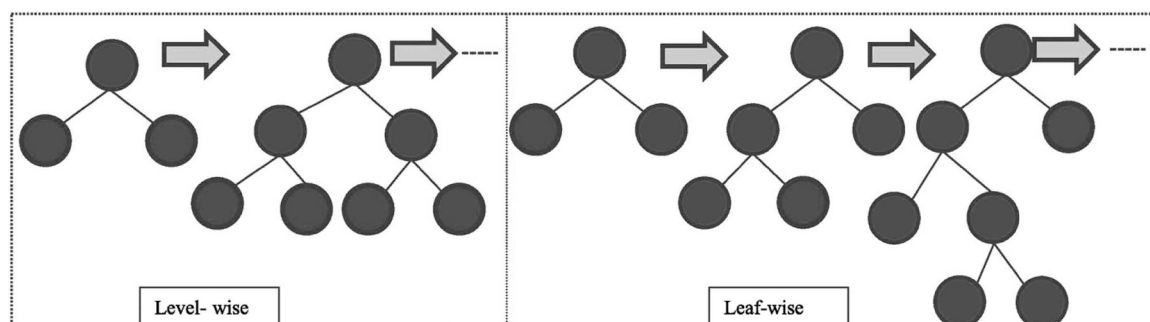


Fig. 10. Construction of decision tree.

capabilities to attain strong predicted accuracy and obtain a full understanding of the data, guaranteeing that our research was meticulous and trustworthy [119–121].

2.2.1. Extreme gradient boosting

XGB model was created as an extension of Friedman's original "Gradient Boosting Machine" model [122]. XGB is a powerful and robust algorithm that can effectively construct ensembles of decision trees, which collaborate and can solve both problems based on classification, and regression. The fundamental issue of this algorithm is to maximize the value of the objective function (OF). Moreover, it applies ML methods within a framework that is strengthened by gradient techniques. Consequently, XGB can efficiently and precisely address

numerous challenges by utilizing parallel boost trees. The XGB algorithm employs a particular technique known as gradient boosting (GB) with regularization, which tackles problems to mitigate overfitting [123–125]. Furthermore, the OF is the addition of all the key index, and the loss function. The loss function measures the difference between values between the experimental and predicted one. While, the regularization factor penalizes the complexity of models. Moreover, Fig. 8 illustrates the entire prediction process of XGB. Initially, the model begins by employing a solitary decision tree. Next, calculate the errors (discrepancies) between the model values and with actual values. Once the error has been calculated, a new decision tree is trained specifically to rectify the faults created by the prior decision tree. Additionally, a novel tree is incorporated into the collection, and the assessed values are

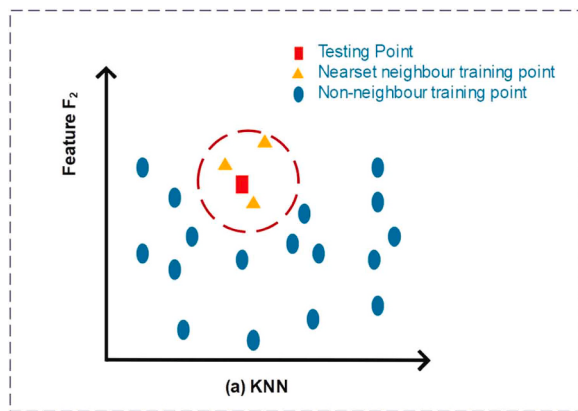


Fig. 11. Schematic diagram of KNN model.

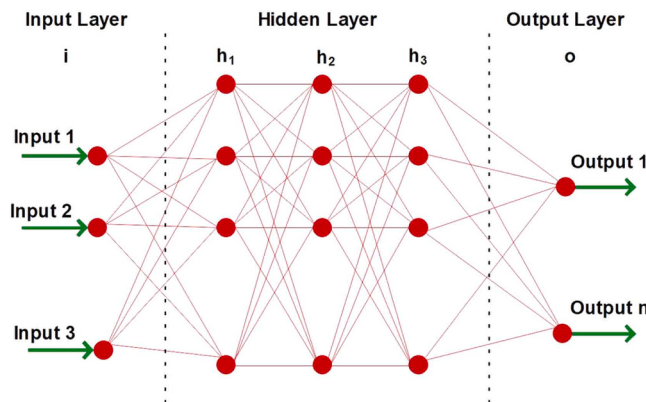


Fig. 12. ANN approach schematic diagram.

revised by integrating the estimations from all the trees in the ensemble. The process of calculating the remaining error and incorporating new trees into the ensemble is repeated until a stopping requirement is satisfied.

2.2.2. Light gradient boosting machine (LightGBM)

Light GBM is a kind of Gradient Boosting Decision Tree that is based on a decision-tree algorithm developed by Microsoft Research [126–128]. Light GBM is a robust method for addressing regression, classification, and other machine-learning problems. It utilizes less memory and surpasses in terms of prediction accuracy. The objective is to enhance computational performance to more efficiently tackle complex data prediction issues [129]. The Light GBM algorithm incorporates two novel techniques: gradient-based one-side sampling (GOSS), designed to handle huge datasets, and exclusive features bundling (EFB), aimed at managing a large number of data features without overfitting issues. Light GBM improves training and reduces memory usage by utilizing the histogram method and the tree leaf-wise growth strategy. The following decimal numbers are partitioned into smaller categories. Subsequently, the histogram is constructed using these bins, taking into account their width. The necessary statistics (sum of gradients and count of samples in each bin) are obtained from the histogram during the initial examination of the data. The optimal segmentation point can be ascertained by analyzing the discrete value of the histogram [130–132]. This strategy can help decrease the expenses associated with storage and measurement. Fig. 9 illustrates the level-wise and leaf-wise development approaches. According to the level-wise growth technique, the leaves on the same layer are divided simultaneously. It is more advantageous to optimize using a large number of threads while also managing the complexity of the model. In addition, the leaves on the same layer are

Table 3
Parameters for making models.

Model	Hyper-parameter	Range	Optimal value
Extreme Gradient Boosting	Learning Rate	0.01–0.3	0.09
	Max Depth	3–10	6
	Subsample	0.5–1	0.8
	Colsample_bytree	0.5–1	0.8
	Number of Estimators (n_estimators)	100–1000	200
	Gamma	0–0.1	0
	Min Child Weight	1–10	1
	Learning Rate	0.01–0.3	0.08
	Max Depth	–1 (no limit) – 15	12
	Number of Leaves	31–128	31
	Min Data in Leaf	20–100	20
	Feature Fraction	0.6–1	0.6
	Bagging Fraction	0.6–1	0.4
	Bagging Frequency	0–5	5
	Number of Estimators (n_estimators)	100–1000	150
LightGBM	Number of Neighbors (n_neighbors)	3–20	5
	Weight Function	uniform, distance	distance
	Algorithm	auto, ball_tree, kd_tree, brute	auto
	Leaf Size	20–50	30
	Number of Layers	1–5	2
Artificial Neural Network	Number of Neurons per Layer	0–250	50
	Learning Rate	0.001–0.01	0.001
	Batch Size	0–150	32
	Activation Function	ReLU, Tanh, Sigmoid	ReLU
	Optimizer	Adam, SGD	Adam
	Number of Epochs	50–200	100
	Dropout Rate	0–0.5	0.2

Table 4
Parameters evaluation criteria on compressive strength.

Indicator used	Range	Reference
$R^2 = \frac{\sum_{i=1}^n (Y_i - \bar{Y}_i)^2}{\sum_{i=1}^n (Y_i - \bar{Y}_i)^2}$	Close to 1	[144]
$RMSE = \sqrt{\frac{\sum_{i=1}^n (P_i - E_i)^2}{N}}$	MAE < RMSE	[145]
$MAE = \frac{1}{n} \sum_{i=1}^n E_i - P_i $		[146]

P_i = predicted data,
 n = data points
 \bar{E}_i = average experiment values

E_i = Experimental data,
 \bar{P}_i = average predicted values,

thoroughly processed, even though they possess distinct information acquisition. The information gain quantifies the expected reduction in entropy that occurs when the nodes are divided based on properties that may be inferred [133].

The leaf-wise development strategy is very effective since it only divides the leaf with the highest information gain at the same level Fig. 10. Moreover, by employing this method, it is possible to generate trees with a significant level of complexity; however, to prevent the model from becoming too specialized for the training data, a maximum depth restriction is enforced throughout the construction of the tree [133].

2.2.3. K-nearest neighbor

K closest neighbor (KNN) is a method that involves making predictions for new data points by comparing them to the most comparable records in a collection. Fig. 11 depicts schematic representations of KNN algorithms. Both regression and classification techniques in machine learning can be utilized. The K-nearest neighbors (KNN) algorithm



Fig. 13. K-fold cross-validation process.

assumes that observations that are proximate in the attribute space (i.e., concrete mix) are also proximate in the output value space [134]. The anticipated output values are determined by a predetermined function that considers the response value of the nearest neighbor in the data space. In the case of standard KNN, the average function is typically employed [134]. The properties of a standard K-nearest neighbors (KNN) algorithm are as follows: 1. Apply equal weighting to all neighboring observations and utilize the average function to determine the response value of unknown data; 2. Assign equal weighting to all characteristics by assuming that all normalized attributes hold equal significance; 3. Employ Euclidean distances to compute the distance [135]. KNN has the advantage of being less influenced by noise present in the training data, making it a useful algorithm for handling enormous volumes of training data.

2.2.4. Artificial neural network

ANNs are complex systems consisting of interconnected components that function in parallel to solve complex issues by deploying artificial neurons [136–138]. An artificial neural network (ANN) is a statistical learning system that draws inspiration from biological neural networks. The Artificial Neural Network (ANN) model is comprised of a multitude of intricately linked neurons. The architecture of artificial neural networks (ANNs) is based on the structure and operation of biological neural networks [139]. An Artificial Neural Network (ANN) consists of neurons that are structured into numerous layers, mirroring the organization of neurons in the human brain. The feedforward neural network is a commonly encountered type of neural network that comprises three layers: an input layer for receiving external data necessary for pattern recognition, an output layer for producing the response, and a hidden layer that connects the other layers [140]. Acyclic arcs connect neighboring neurons in the input and output layers. The Artificial Neural Network (ANN) employs a training technique to acquire information from datasets [141]. The neuron's weights are modified according to the mismatch between the expected results and the actual output. This

method is iterated until the error rate is minimized. ANNs often utilize the backpropagation approach as a training tool to extract knowledge from datasets. Fig. 12 depicts the comprehensive architecture of an Artificial Neural Network (ANN) approach.

3. Hyper-parameters tuning

Hyperparameter fine-tuning is essential in ML as it directly affects the performance and efficiency of models [142]. Hyperparameters are configurable factors that determine the behavior and performance of an ML model during training. They include settings like learning rate, batch size, hidden layers, learning rate, etc. Optimizing hyper-parameters can greatly improve a model's capacity to accurately predict outcomes, generalize to new data, and train more efficiently. In contrast, inadequately selected hyper-parameters might result in unsatisfactory performance, overfitting, or under-fitting [143]. Hyper-parameter tuning entails employing systematic search and optimization approaches to determine the optimal parameter configuration for a certain model and dataset. This process guarantees that the model attains its maximum potential and produces dependable and resilient outcomes. Table 3 displays the comprehensive adjustment of the parameters.

4. Statistical analysis

The ML model created for making the prediction of NMs in composite is created based on the dataset should be tested using the data from the testing set. In addition, measure index like Root Mean Square Error (RMSE), Mean Absolute Error (MAE), and co-efficient of determination (R^2) were used to evaluate the model's performance in terms of predicting unseen data to ensure the validity of the results. These metrics highlight/errors between the planned and actual results. Hence, a smaller difference between their values suggests the accuracy of the models [76]. The lower the score the better as this means that the model is making accurate predictions which is a good sign. Therefore, it says that the model can perform almost as well as the real-world data. Moreover, when the values of R and R^2 are closer to 1, the model's predictions are more accurate to account for the total variation in the data. Table 4 shows the statistical measures used in this study.

5. Uncertainty analysis

Uncertainty analysis (UA) is a useful technique that is used to evaluate and compute the ambiguity related with the forecasting accuracy of hybrid machine learning models. When forecasting CS of nanocomposite, it is crucial to acknowledge and handle the uncertainties that occur in prediction algorithms. These uncertainties include those related to experimental data, input predictors, and model results [147]. This method helps in making accurate analysis of the conclusion between results, and enables the researchers by considering the level of improbability in the algorithms (see Eq. 1).

$$U_{95} = 1.96 \sqrt{SD^2 + RMSE^2} \quad (1)$$

The variables "SD" and "1.96" are used to represent the standard deviation and 95 % confidence interval, respectively, of the model's prediction performance error according to a normal distribution.

6. K-fold cross-validation

K-fold cross-validation (CV) is used to develop a model that can perform well on unseen data by assessing the model's accuracy on new data [99]. The flowchart of the K-fold CV is presented in Fig. 13. Initially, the dataset is separated into binary distinct components: the training set and the testing set. At this stage, the testing dataset is kept aside and is used only during the final evaluation where the performance of the model is tested on entirely new data [8]. The training set is then

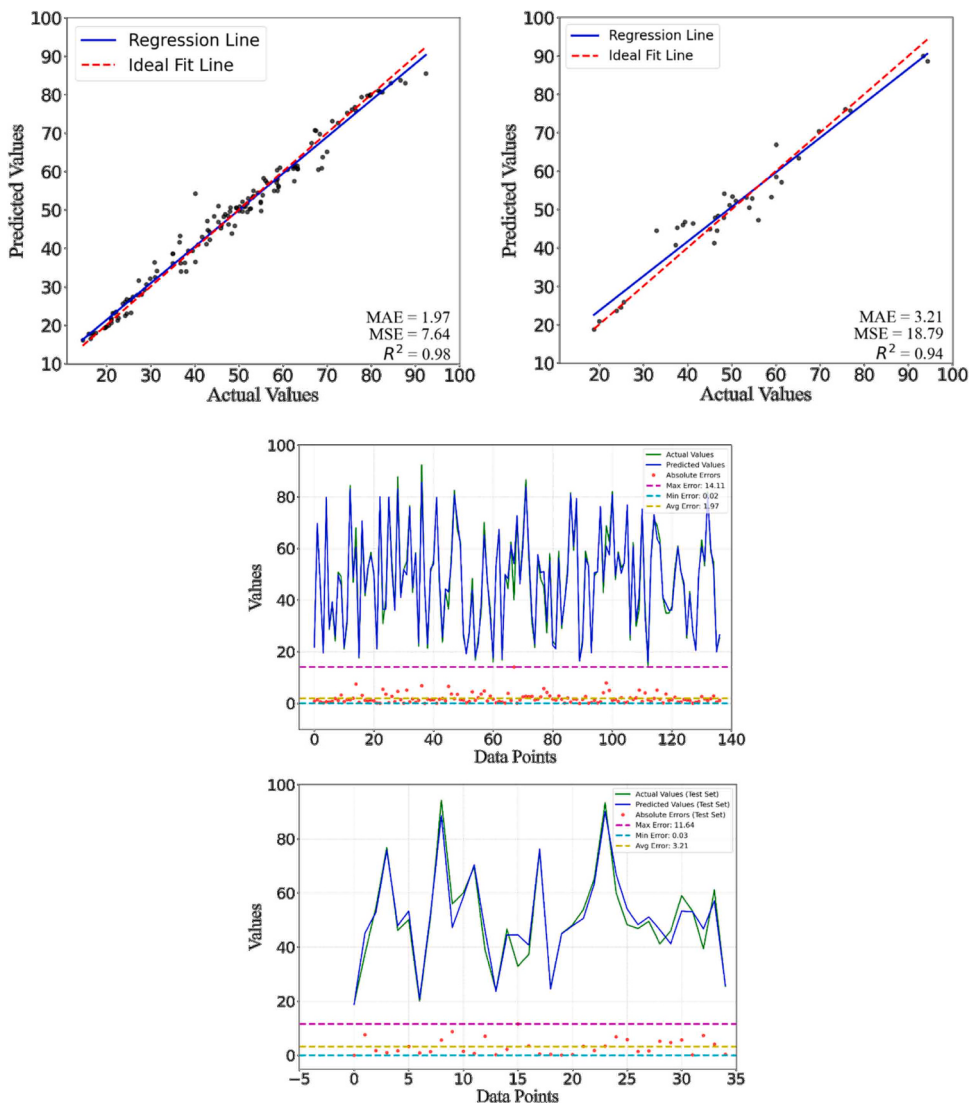


Fig. 14. XGB approach; (a) train R^2 , (b) test R^2 , (c) train discrepancies; (d) test discrepancies.

divided into K subsets (or groups) of equal size with each subset being randomly selected. When one fold is selected as the validation set, the model is trained with the rest of the ($K - 1$) folds. After applying the same procedure for all K folds, the final model score is computed based on the average performance of the model across the K iterations. For this study, the training dataset has been split into ten folds ($K = 10$) based on the guidelines provided by the sources.

7. Result and discussion

7.1. Extreme gradient boosting

XGBoost, a very efficient and high-performing version of gradient boosting, has gained widespread recognition in both machine-learning contests and real-world applications. The software's capacity to manage incomplete data, integrate regularization techniques, and effectively handle extensive datasets makes it a favored option for regression assignments. To get strong and reliable performance in regression tasks, it is crucial to ascertain the most favorable slope of the regression line. The XGBoost model demonstrates strong predictive accuracy in this investigation, as indicated by a notable coefficient of determination (R^2) of 0.98 in the training phase and 0.94 in the testing

phase, as depicted in Fig. 14(a) and Fig. 14(b). The high R^2 values indicate a robust connection between the anticipated and actual values, implying that the model accurately reflects the underlying patterns in the data. The strong correlation between the anticipated results and empirical benchmarks highlights the efficacy of the model. Chen et al. [148] emphasized the exceptional performance of XGBoost in both regression and classification tasks, attributing its success to unique system and algorithmic optimizations. The results obtained from the dataset suggest that the XGBoost model has undergone thorough training, allowing it to effectively generalize to unfamiliar data. Model evaluation is a crucial factor that showcases the model's resilience and dependability in real-world scenarios, extending beyond the data used for training. Furthermore, a comprehensive error analysis of both the train and test set indicates an average error of roughly 1.97 MPa and 3.21 MPa, respectively. The model's error margins vary between 0.03 MPa and 11.64 MPa, as shown in Fig. 14(c) and Fig. 14(d). This analysis suggests that although the model is generally precise, there are occasional discrepancies, which are inherent in most predictive models.

7.2. Light gradient boosting machine

The model initiates by undergoing training on a dataset that has been

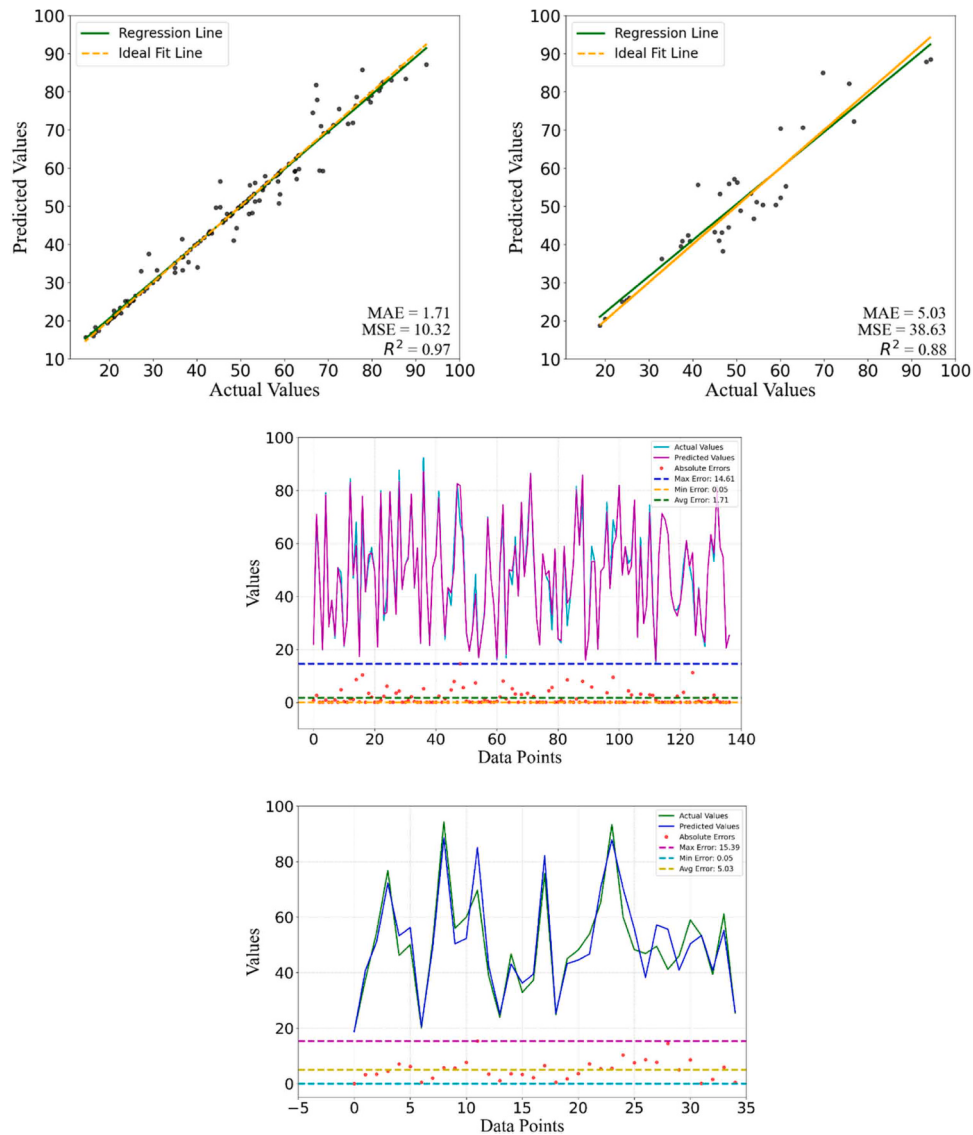


Fig. 15. LGB approach; (a) train R^2 , (b) test R^2 , (c) train discrepancies; (d) test discrepancies.

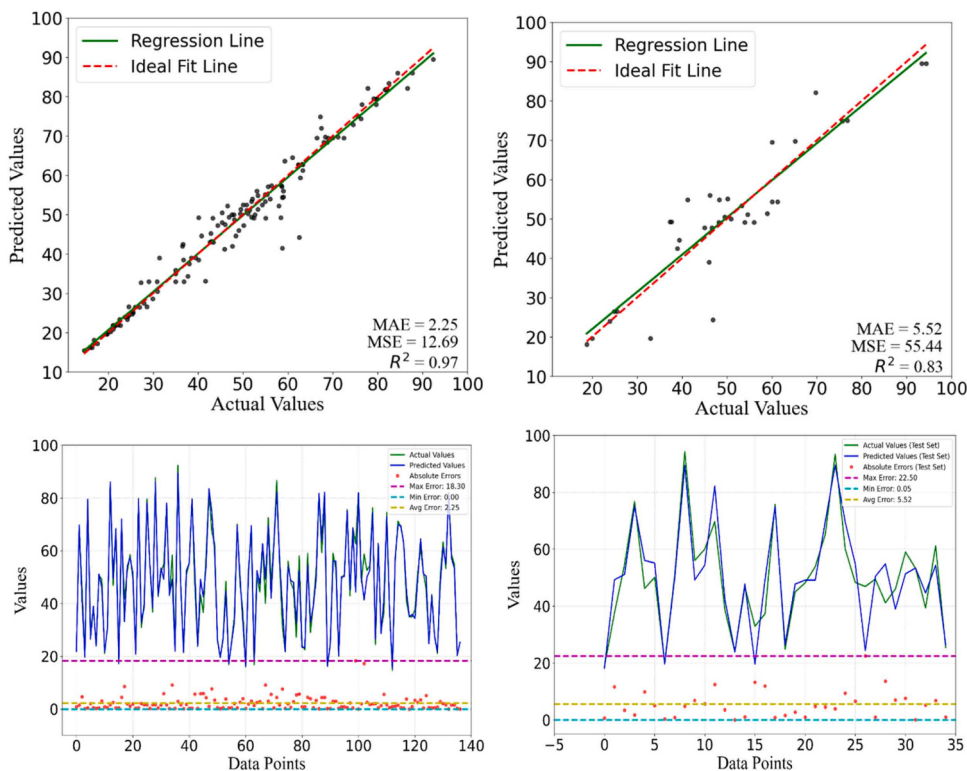


Fig. 16. KNN approach; (a) train R^2 , (b) test R^2 , (c) train discrepancies; (d) test discrepancies.

annotated. This process boosts the model's capability and thus makes accurate predictions by enabling it to identify and understand arrangements and correlations present in the data. This procedure enhances the precision of the model and empowers it to detect possible deficiencies in its forecasts. Furthermore, precise regression models are essential in a wide range of disciplines. In addition, accurate forecasts are essential for the design of experiments, optimization of processes, and making well-informed decisions. The precision and dependability of these models have a direct influence on the excellence of insights and decisions. The training data for the model has a strong correlation of roughly 0.97, as shown in Fig. 15(a). It is important to emphasize that a high correlation within the training sample does not automatically ensure reliable performance on new, unknown data. This problem can occur when the model is excessively intricate and excessively fits the training data. To assess the model's ability to apply its knowledge to new situations, it is necessary to test its performance on previously unseen data, as depicted in Fig. 15(b). The analysis demonstrates the relationship between the empirical observations of nanomaterials derived from various combinations and the expected results of the model. The model demonstrates a commendable level of prediction accuracy, as demonstrated by its correlation score of 0.88. The significant correlation indicates that the model can efficiently apply its knowledge to new data, retaining a high level of accuracy even outside of the training set. Ke et al. [149] emphasized that LightGBM outperforms other boosting methods in terms of managing large-scale data and delivering faster training speeds. Figs. 15(c) and 15(d) display the scattering of empirical points from different mixtures in comparison to the forecasts generated by the model. Upon analyzing the test set, it was found that the errors were distributed with a maximum error of 15.39 MPa, a minimum error of 0.05 MPa, and an average error of 5.03 MPa.

7.3. K-nearest neighbors

Fig. 16 displays the outcomes of the K-Nearest Neighbors (KNN) model on both the training and test sets of nanomaterial-based concrete.

The model underwent training using an 80/20 split ratio, a commonly employed technique to assure reliable performance by allocating a substantial amount of data for training while saving a large fraction for testing purposes. In the field of machine learning, the term "training data" refers to the initial information that is utilized to teach the model to recognize patterns or accomplish particular goals. Testing, however, is employed to assess the model's precision and effectiveness on data that has not been previously seen. Understanding this differentiation is essential for evaluating the model's ability to apply its knowledge to new data beyond its training set. Fig. 16(a) depicts the relationship between the observed and predicted results for the training dataset, indicating a strong coefficient of determination ($R^2 = 0.97$). As the model undergoes training, it acquires the ability to recognize intricate patterns and correlations within the data. It utilizes this acquired knowledge to generate forecasts on novel, unobserved data. Through the process of making adjustments and rectifying errors during training, the model enhances its ability to accurately anticipate outcomes. Fig. 16(b) demonstrates the equilibrium by illustrating the correlation between variables for the test set, with an R^2 value of around 0.83. Fig. 16(c) displays the distribution of bias in the training set based on its mistakes. A model that exhibits a strong correlation between variables in the training dataset does not necessarily ensure good predictions on fresh data, as there is a risk of overfitting. Overfitting arises when a model becomes excessively intricate and begins to incorporate irrelevant noise and random variations from the training data, rather than focusing on the fundamental patterns. This leads to inadequate extrapolation to unfamiliar data. To prevent overfitting, it is essential to strike a balance between the complexity of the model and its capacity to generalize to unfamiliar data. Fig. 16(d) displays the graphical representation of the error distribution for the test set, with an average error value of around 5.52 MPa. The research demonstrates that the model exhibits consistent performance on both the training and test sets, with minimal variation in error measures.

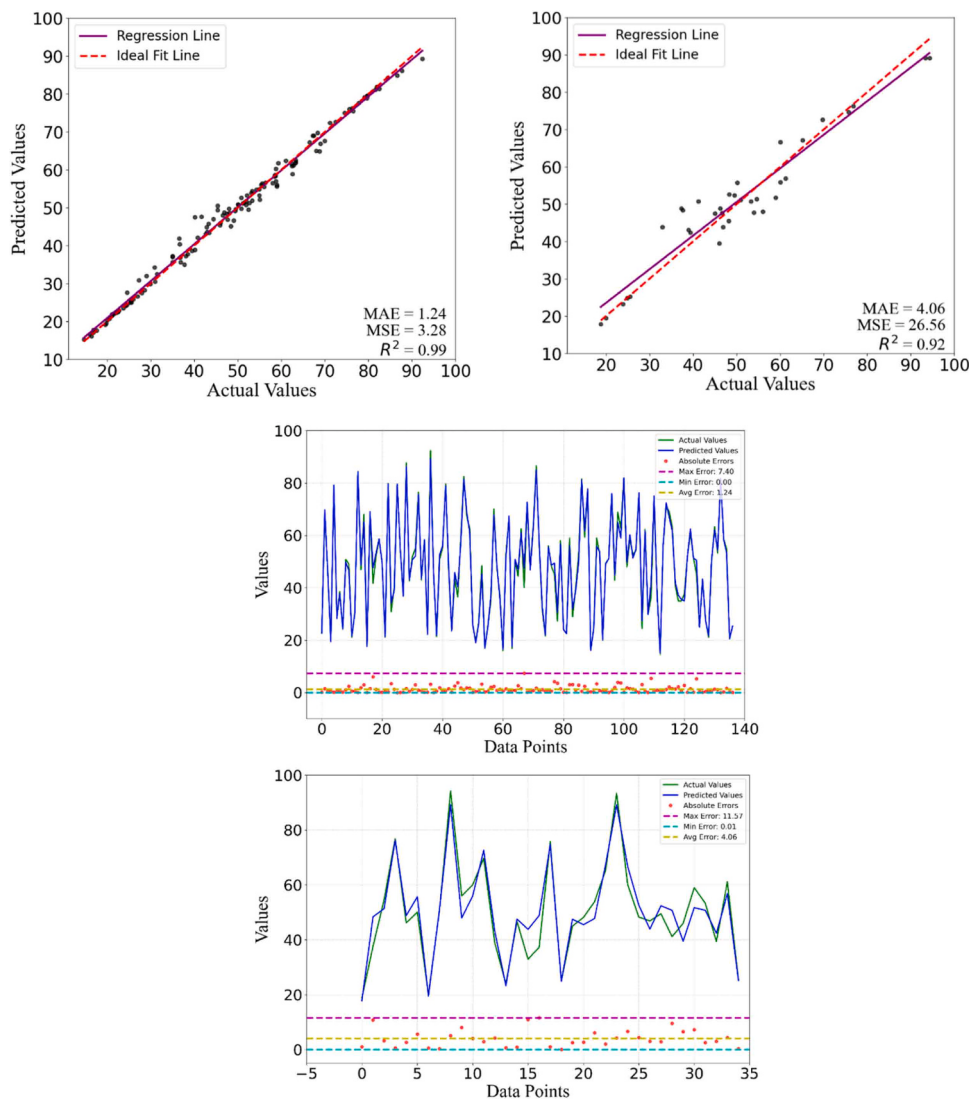


Fig. 17. ANN approach; (a) train R^2 , (b) test R^2 , (c) train errors; (d) test discrepancies.

Table 5
Displays the performance metrics for all of the models.

Approaches	Extreme gradient boosting	Light gradient boosting	K-Nearest Neighbors	Artificial neural network
Training				
R^2	0.98	0.97	0.96	0.99
RMSE	2.763	3.212	3.563	1.812
MAE	1.972	1.71	2.247	1.24
Testing				
R^2	0.94	0.88	0.839	0.918
RMSE	4.335	6.21	7.446	5.513
MAE	3.21	5.03	5.524	4.058

7.4. Artificial neural network

The artificial neural network (ANN) model exhibits robust prediction capabilities. The model attains a significant R^2 coefficient of determination of 0.99 during the training process as demonstrated in Fig. 17(a). Therefore, this suggests a robust link between the projected and real values. The testing phase, with an R^2 value of 0.92, demonstrates that the model maintains a high level of performance when applied to fresh and previously unseen data as illustrated in Fig. 17(b). The error analysis verifies that the model's predictions are exceedingly precise for the

majority of instances, with the bulk of errors being less than 10 MPa. Furthermore, Fig. 17(c) and Fig. 17(d) illustrate the distribution of colored data points with discrepancies, representing empirical observations from various mixtures, in contrast to the expected outcomes predicted by the ANN model. The outcomes also provide statistics on error discrepancies for the train and test set, highlighting the maximum, minimum, and average values for the particular samples as 11.57 MPa, 0.01 MPa, and 4.06 MPa, respectively (see Fig. 17(d)).

7.5. Performance metrics of ML models

The accurateness of a prediction model is commonly assessed using performance measures such as R^2 , root mean square error (RMSE), and mean absolute error (MAE). These indexes mostly rely on evaluating the disparities between forecast, and experimental values. Table 5 displays the performance metrics for all of the approaches. Furthermore, Fig. 18 depicts a radar graph that showcases all the models together with their respective error values.

7.6. Uncertainty analysis

Uncertainty analysis is essential for managing the ambiguity in a models that are used to forecast the prediction of CS of nanocomposite. This helps in assessing the reliability and robustness of the models. The

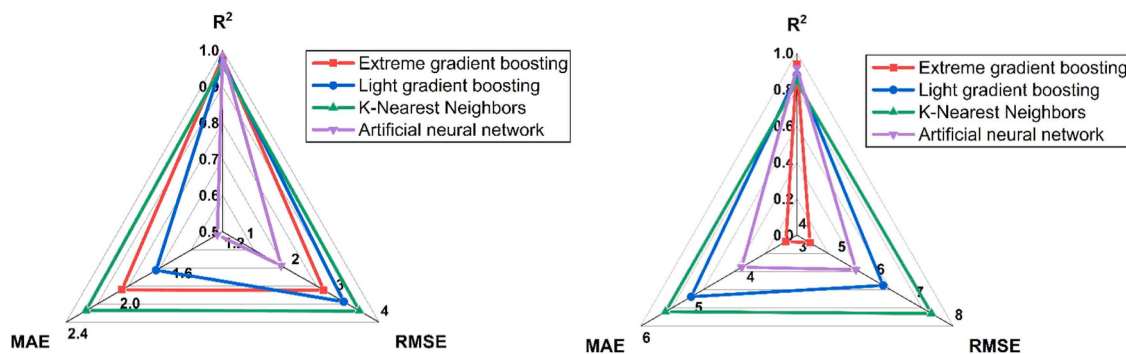


Fig. 18. Radar graph of models.

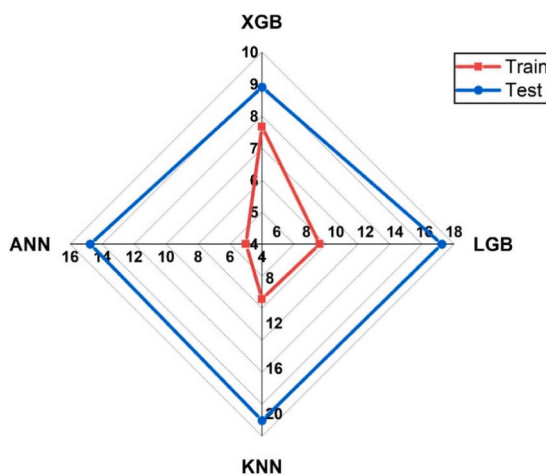


Fig. 19. Uncertainty analysis of models.

uncertainty analysis test result for nanocomposite in the testing and training phases is presented in Fig. 19. It can be seen that XGB model exhibit least level of ambiguity for train and test set. The train and test set for XGB, LGB, KNN, and ANN models demonstrate 7.668 %, 8.9 %, 8.9 %, 17.18 %, 9.85 %, 20.61, and 5 %, 14.74 %, respectively. This is due to the robust performance of XGB as it prevents noise, and overfitting of the entire data. Amir et al. [150] reveals that the models uncertainty falls below the 35 % threshold. Hence, according to our findings, the performance of these entities can be deemed robust since it is below the 21 % level.

7.7. K-fold cross-validation

The approach is useful in ML as it reduces overfitting, give better generalization, reduces variance as it divides the overall data into ten groups. These ten set consist of subsets with nine set used for training, and one set is reserved for validation. The precision of a model was assessed based on lower error values for metrics such as Mean Absolute Error (MAE) and Root Mean Square Error (RMSE), as well as greater R^2 values. To ensure the dependability of the findings and facilitate precise decision-making, this procedure was iterated ten times to achieve a resilient analysis. Thanks to this extensive endeavor, the models achieved a notable degree of accuracy. Fig. 20 depicts the

comprehensive validation analysis of models containing the aforementioned flaws. The approaches demonstrate a substantial improvement in the models, as seen by lower average errors and higher correlation. Therefore, the use of validation in the 10-K series shows a substantial response for each model.

7.8. Feature importance

Feature significance is a critical aspect of machine learning as it enables the identification of the features or variables that have the most substantial influence on the output of a prediction model. This methodology not only improves the reliability of our results but also enables us to make well-informed choices based on evidence-based insights, leading to progress in our area as shown in Fig. 21. The thickness of graphene nanoplatelets (GNP) is a critical factor in defining the mechanical characteristics and reinforcing efficacy of the nanocomposite. Increased thickness of graphene nanoplatelets (GNPs) can enhance load transfer and distribution within the concrete matrix. Thus, leading to a substantial improvement in the overall strength and longevity of the composite. The size of GNPs affects their surface area and their interaction with the cement matrix. Increased diameters generally lead to a larger surface area for stress transmission. Hence, improving the mechanical characteristics of the composite material. Furthermore, the size of GNPs influences the distribution and orientation of the particles, which in turn affects the overall performance of the nanocomposite. Similarly, the process of curing concrete is crucial for the enhancement of its mechanical qualities. Over time, the process of hydration persists, resulting in enhanced strength and durability. The curing duration has an impact on the extent to which the GNPs can merge with the cement matrix and enhance the overall characteristics of the nanocomposite. Sonication is employed to provide a homogeneous dispersion of GNPs within the cement matrix. Effective dispersion is crucial for ensuring the even distribution of GNPs, which prevents the formation of clusters and enhances their ability to reinforce. In addition, sand is a crucial ingredient in concrete, yet its influence on the characteristics of GNP-reinforced nanocomposites is rather minor when compared to other elements. Sand mainly influences the ability to work with and the fundamental mechanical properties of concrete. However, its impact on GNP reinforcement is quite insignificant, as shown in Fig. 21.

7.9. Graphical user interface

This section outlines the process of creating a user-friendly graphical user interface (GUI) as illustrated in Fig. 22. The GUI has a toolbar, an

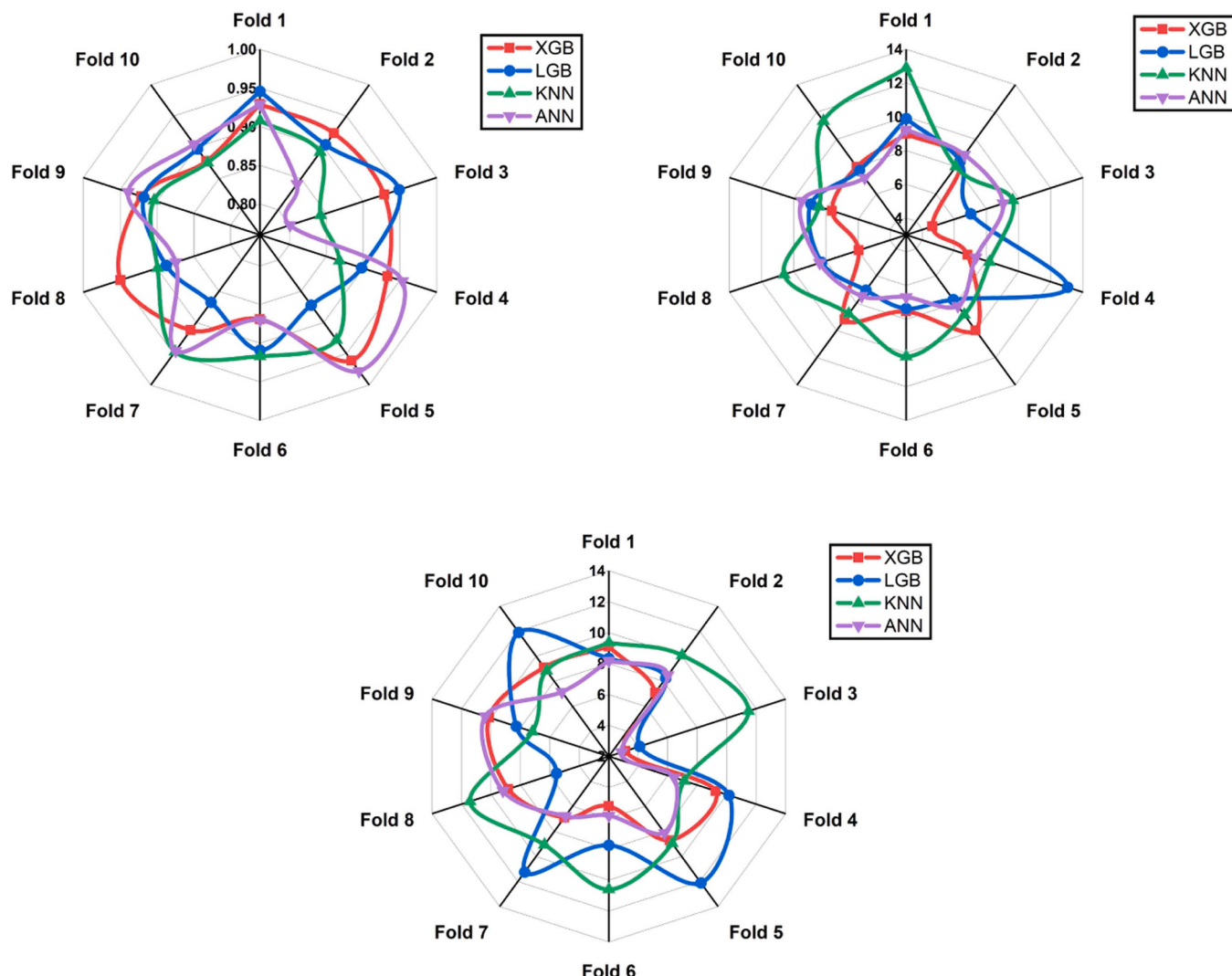


Fig. 20. Fold analysis result; (a) R^2 , (b) RMSE, (c) MAE.

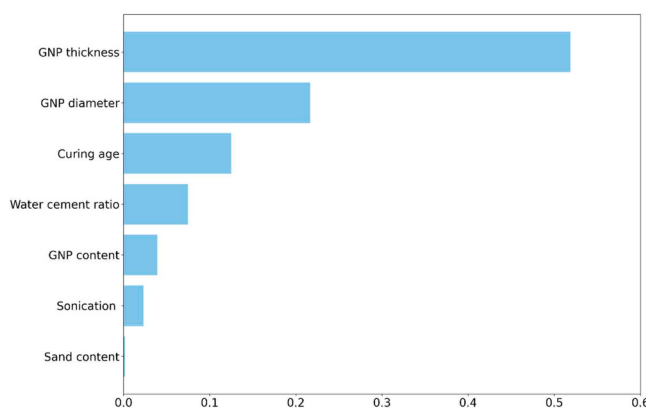


Fig. 21. Feature importance of the parameters in nanocomposite.

input section, and an output section. It is also easy for the researchers to key in the seven variables into the provided input box. Users can get the predicted values of nanocomposite by clicking on the “Predict” button located in the output section. The input section contains seven factors that affect the nanomaterial concrete strength. This graphical user interface (GUI) can be used by engineers to create concrete that best

suits the specific needs and challenges of building construction. The graphical user interface (GUI) was developed to ensure ease of use in the analysis and prediction of nano material-CS behavior for researchers. Moreover, this research aims to provide researchers with a tool that would help them to fully harness the potential of the proposed paradigm in their work by developing this GUI.

8. Conclusions

The objective of this project is to develop machine-learning prediction models for nanocomposites that incorporate graphene. The study utilizes four different machine learning (ML) techniques, namely as ANN, XGB, LGB, and KNN to develop a precise prediction model for the composite matrix. To construct these models, a total of 172 data points were collected from published studies. These data points included seven important input factors and the output variable considered was the CS. The accurateness of the models was evaluated using statistical measures and k-fold validation. Furthermore, the subsequent conclusions can be made.

1. The extreme gradient boosting and artificial neural network technique demonstrate a high degree of accuracy by achieving R^2 values of more than 0.9 for both the training and testing phases, aligning well with both modeled and experimental results. The models

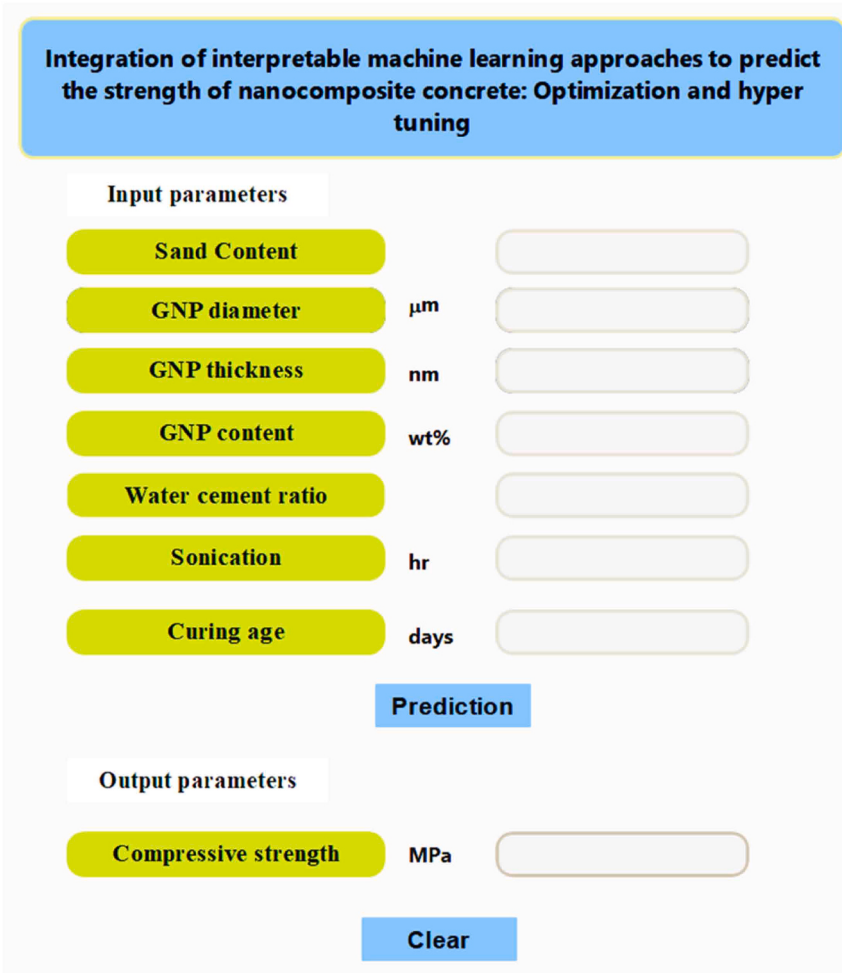


Fig. 22. GUI of nanocomposite.

- created using XGBoost and ANN approaches exhibit a remarkable level of precision. Thus, indicating their ability to accurately predict outcomes based on the training data and effectively generalize to unseen data during the testing phase.
- The XGB model demonstrates robust performance by showing lesser statistical index (MAE, RMSE, and R^2), as compared to remaining models. Moreover, ANN, and LGB also show lesser measures but XGB model demonstrates superior performance.
 - The models were evaluated using statistical metrics by K-fold cross-validation. The analysis depicts that all models exhibits a stronger correlation (R^2) with minimal statistical indexes (MAE, RMSE). In addition, deviations with ten folds are also observed but models show superior results. In addition, uncertainty analysis reveals that all models show less level of ambiguity for train and test set. The train and test set for XGB, LGB, KNN, and ANN models demonstrate 7.668 %, 8.9 %, 8.9 %, 17.18 %, 9.85 %, 20.61, and 5 %, 14.74 %, respectively
 - The feature analysis indicated that the GNP thickness, diameter, and age component parameters exerted the most significant influence on forecasting the intended output. The enhanced strength is a result of the improved load transfer, increased surface area, and hydration provided by GNP particles.
 - The development of GUI aimed to optimize the productivity of academics and professionals by offering them a user-friendly, streamlined, and visually-oriented interface. By doing this, it improves both the effectiveness and efficiency of work and production.

CRediT authorship contribution statement

Turki S. Alahmari: Writing – review & editing, Writing – original draft, Methodology, Investigation, Funding acquisition, Formal analysis, Data curation, Conceptualization. **Kiran Arif:** Conceptualization, Formal analysis, Supervision, Writing – review & editing.

Declaration of Competing Interest

The authors declare that they have no known competing financial interests or personal relationships that could have appeared to influence the work reported in this paper.

Data availability

Data will be made available on request.

References

- H. Lin, Y. Han, S. Liang, F. Gong, S. Han, C. Shi, P. Feng, Effects of low temperatures and cryogenic freeze-thaw cycles on concrete mechanical properties: a literature review, *Constr. Build. Mater.* 345 (2022), <https://doi.org/10.1016/j.conbuildmat.2022.128287>.
- Z. Liu, Z. Xu, X. Zheng, Y. Zhao, J. Wang, 3D path planning in threat environment based on fuzzy logic, *J. Intell. Fuzzy Syst.* 46 (2024) 7021–7034, <https://doi.org/10.3233/JIFS-232076>.
- R. Rakesh Kumar Reddy, S.C. Yaragal, V.K. Sanjay, Processing of laboratory concrete demolition waste using ball mill, *Mater. Today Proc.* (2023), <https://doi.org/10.1016/j.matpr.2023.03.193>.

- [4] J. Bernal, M. Fenaux, A. Moragues, E. Reyes, J.C. Gálvez, Study of chloride penetration in concretes exposed to high-mountain weather conditions with presence of deicing salts, *Constr. Build. Mater.* 127 (2016) 971–983, <https://doi.org/10.1016/j.conbuildmat.2016.09.148>.
- [5] J. Wei, H. Ying, Y. Yang, W. Zhang, H. Yuan, J. Zhou, Seismic performance of concrete-filled steel tubular composite columns with ultra high performance concrete plates, *Eng. Struct.* 278 (2023), <https://doi.org/10.1016/j.engstruct.2022.115500>.
- [6] L. Sun, C. Wang, C. Zhang, Z. Yang, C. Li, P. Qiao, Experimental investigation on the bond performance of sea sand coral concrete with FRP bar reinforcement for marine environments, *Adv. Struct. Eng.* (2022), <https://doi.org/10.1177/1369432221131153>.
- [7] A. Akbar, F. Farooq, M. Shafique, F. Aslam, R. Alyousef, H. Alabduljabbar, Sugarcane bagasse ash-based engineered geopolymers mortar incorporating propylene fibers, *J. Build. Eng.* 33 (2021) 101492, <https://doi.org/10.1016/j.jobe.2020.101492>.
- [8] F. Farooq, W. Ahmed, A. Akbar, F. Aslam, R. Alyousef, Predictive modeling for sustainable high-performance concrete from industrial wastes: a comparison and optimization of models using ensemble learners, *J. Clean. Prod.* 292 (2021) 126032, <https://doi.org/10.1016/j.jclepro.2021.126032>.
- [9] H. He, E. Shuang, D. Lu, Y. Hu, C. Yan, H. Shan, C. He, Deciphering size-induced influence of carbon dots on mechanical performance of cement composites, *Constr. Build. Mater.* 425 (2024), <https://doi.org/10.1016/j.conbuildmat.2024.136030>.
- [10] C. Chen, D. Han, C.C. Chang, MPCCT: multimodal vision-language learning paradigm with context-based compact Transformer, *Pattern Recognit.* 147 (2024), <https://doi.org/10.1016/j.patcog.2023.110084>.
- [11] M.L. Nehdi, A. Marani, L. Zhang, Is net-zero feasible: systematic review of cement and concrete decarbonization technologies, *Renew. Sustain. Energy Rev.* 191 (2024) 114169, <https://doi.org/10.1016/j.rser.2023.114169>.
- [12] B. Joshi, P. Sudhakaran, M. Varma, A. Saxena, Partial replacement of cement and fine aggregate in mortar material by using carbon sequestration technique, *Mater. Today Proc.* (2023), <https://doi.org/10.1016/j.matpr.2023.03.649>.
- [13] J. Chen, Y. Ji, Y. Xu, G. Wang, K. Hu, Experimental investigation of behavior of reinforced high-strength concrete walls under standard fire, *J. Build. Eng.* 87 (2024), <https://doi.org/10.1016/j.jobe.2024.109052>.
- [14] C. Chen, D. Han, X. Shen, CLVIN: Complete language-vision interaction network for visual question answering, *Knowl.-Based Syst.* 275 (2023), <https://doi.org/10.1016/j.knosys.2023.110706>.
- [15] Y.R. Alharbi, A.A. Abadel, O.A. Mayhoub, M. Kohail, Effect of using available metakaoline and nano materials on the behavior of reactive powder concrete, *Constr. Build. Mater.* 269 (2021) 121344, <https://doi.org/10.1016/j.conbuildmat.2020.121344>.
- [16] M.O. Mohsen, M.M. Al-Diseet, M.O. Aburumman, M. Abdel-Jaber, R. Taha, M. S. Al Ansari, A.A. Taqa, Hybrid effect of GNPs, GOs, and CNTs on the flexural and compressive strengths of cement paste, *J. Build. Eng.* 73 (2023), <https://doi.org/10.1016/j.jobe.2023.106679>.
- [17] A. Khalid, R.A. Khushnood, A. Mahmood, G.A. Ferro, S. Ahmad, Synthesis, characterization and applications of nano/micro carbonaceous inerts: a review, in: *Procedia Struct. Integr.*, Elsevier, 2018, pp. 116–125, <https://doi.org/10.1016/j.prostr.2018.06.019>.
- [18] L. Dyshlyuk, O. Babich, S. Ivanova, N. Vasilchenko, V. Atuchin, I. Korolkov, D. Russakov, A. Prosekov, Antimicrobial potential of ZnO, TiO₂ and SiO₂ nanoparticles in protecting building materials from biodegradation, *Int. Biodeterior. Biodegrad.* 146 (2020) 104821, <https://doi.org/10.1016/j.ibiod.2019.104821>.
- [19] H. Huang, M. Huang, W. Zhang, S. Pospisil, T. Wu, Experimental Investigation on Rehabilitation of Corroded RC Columns with BSP and HPFL under Combined Loadings, *J. Struct. Eng.* 146 (2020), [https://doi.org/10.1061/\(asce\)st.1943-541x.000275](https://doi.org/10.1061/(asce)st.1943-541x.000275).
- [20] H. Huang, M. Guo, W. Zhang, J. Zeng, K. Yang, H. Bai, Numerical investigation on the bearing capacity of RC columns strengthened by HPFL-BSP under combined loadings, *J. Build. Eng.* 39 (2021), <https://doi.org/10.1016/j.jobe.2021.102266>.
- [21] F. Farooq, A. Akbar, R.A. Khushnood, Effect of hybrid carbon nanotubes/graphite nano platelets on mechanical properties of cementitious composite, in: *Proc. of the First Conf. Sustain. Civ. Eng.* (2019).
- [22] H. Huang, Y. Yuan, W. Zhang, M. Li, Seismic behavior of a replaceable artificial controllable plastic hinge for precast concrete beam-column joint, *Eng. Struct.* 245 (2021), <https://doi.org/10.1016/j.engstruct.2021.112848>.
- [23] D. Lu, G. Wang, X. Du, Y. Wang, A nonlinear dynamic uniaxial strength criterion that considers the ultimate dynamic strength of concrete, *Int. J. Impact Eng.* 103 (2017) 124–137, <https://doi.org/10.1016/j.ijimpeng.2017.01.011>.
- [24] S. Özén, B. Alam, Compressive strength and microstructural characteristics of natural zeolite-based geopolymers, *Period. Polytech. Civ. Eng.* 62 (2018) 64–71, <https://doi.org/10.3311/PPci.10848>.
- [25] D. Cui, L. Wang, C. Zhang, H. Xue, D. Gao, F. Chen, Dynamic Splitting Performance and Energy Dissipation of Fiber-Reinforced Concrete under Impact Loading, *Mater. (Basel)* 17 (2024), <https://doi.org/10.3390/ma17020421>.
- [26] D. Lu, X. Zhou, X. Du, G. Wang, A 3D fractional elastoplastic constitutive model for concrete material, *Int. J. Solids Struct.* 165 (2019) 160–175, <https://doi.org/10.1016/j.ijsolstr.2019.02.004>.
- [27] R. Zhao, C. Li, X. Guan, Advances in modeling surface chloride concentrations in concrete serving in the marine environment: a mini review, *Buildings* 14 (2024), <https://doi.org/10.3390/buildings14061879>.
- [28] W. Meng, K.H. Khayat, Mechanical properties of ultra-high-performance concrete enhanced with graphite nanoplatelets and carbon nanofibers, *Compos. Part B Eng.* 107 (2016) 113–122, <https://doi.org/10.1016/j.compositesb.2016.09.069>.
- [29] A. Sedaghatdoost, K. Behfarnia, Mechanical properties of Portland cement mortar containing multi-walled carbon nanotubes at elevated temperatures, *Constr. Build. Mater.* 176 (2018) 482–489, <https://doi.org/10.1016/j.conbuildmat.2018.05.095>.
- [30] S. He, J. Chai, Y. Yang, J. Cao, Y. Qin, Z. Xu, Effect of nano-reinforcing phase on the early hydration of cement paste: a review, *Constr. Build. Mater.* 367 (2023), <https://doi.org/10.1016/j.conbuildmat.2022.130147>.
- [31] G. Chen, M. Yang, L. Xu, Y. Zhang, Y. Wang, Graphene nanoplatelets impact on concrete in improving freeze-thaw resistance, *Appl. Sci.* 9 (2019), <https://doi.org/10.3390/app9173582>.
- [32] Y.-H. Chen, S.-C. Lin, J.-A. Wang, S.-Y. Hsu, C.-C.M. Ma, Preparation and properties of graphene/carbon nanotube hybrid reinforced mortar composites, *Mag. Concr. Res.* (2018) 1–13, <https://doi.org/10.1680/jmacr.18.00070>.
- [33] T.T. Win, L. Prasitisopin, P. Jongvivatsakul, S. Likitlersuang, Investigating the synergistic effect of graphene nanoplatelets and fly ash on the mechanical properties and microstructure of calcium aluminate cement composites, *J. Build. Eng.* 78 (2023), <https://doi.org/10.1016/j.jobe.2023.107710>.
- [34] J. Shao, H. Zhu, B. Zhao, S.I. Haruna, G. Xue, W. Jiang, K. Wu, J. Yang, Combined effect of recycled tire rubber and carbon nanotubes on the mechanical properties and microstructure of concrete, *Constr. Build. Mater.* 322 (2022) 126493, <https://doi.org/10.1016/j.conbuildmat.2022.126493>.
- [35] J. Wang, S. Dong, S.D. Pang, C. Zhou, B. Han, Pore structure characteristics of concrete composites with surface-modified carbon nanotubes, *Cem. Comcr. Compos.* 128 (2022) 104453, <https://doi.org/10.1016/j.cemconcomp.2022.104453>.
- [36] Y. Gao, H. Jing, Z. Yu, L. Li, J. Wu, W. Chen, Particle size distribution of aggregate effects on the reinforcing roles of carbon nanotubes in enhancing concrete ITZ, *Constr. Build. Mater.* 327 (2022) 126964, <https://doi.org/10.1016/j.conbuildmat.2022.126964>.
- [37] Z. Hu, L. Mao, J. Xia, J. Liu, J. Gao, J. Yang, Q. Liu, Five-phase modelling for effective diffusion coefficient of chlorides in recycled concrete, *Mag. Concr. Res.* 70 (2018) 583–594, <https://doi.org/10.1680/jmacr.17.00194>.
- [38] K.H. Mo, T.C. Ling, Q. Cheng, Examining the Influence of Recycled Concrete Aggregate on the Hardened Properties of Self-compacting Concrete, Waste Biomass--. Valoriz. 12 (2021) 1133–1141, <https://doi.org/10.1007/s12649-020-01045-x>.
- [39] F. Ren, J. Mo, Q. Wang, J.C.M. Ho, Crumb rubber as partial replacement for fine aggregate in concrete: an overview, *Constr. Build. Mater.* 343 (2022), <https://doi.org/10.1016/j.conbuildmat.2022.128049>.
- [40] K. Sargunan, M. Venkata Rao, A. Alex Rajesh, R. Babu, P. Prasanthini, K. Jagadeep, M.L. Rinawa, Experimental investigations on mechanical strength of concrete using nano-alumina and nano-clay, *Mater. Today Proc.* 62 (2022) 5420–5426, <https://doi.org/10.1016/j.matpr.2022.03.703>.
- [41] W. Zhang, X. Liu, Y. Huang, M.N. Tong, Reliability-based analysis of the flexural strength of concrete beams reinforced with hybrid BFRP and steel rebars, *Arch. Civ. Mech. Eng.* 22 (2022), <https://doi.org/10.1007/s43452-022-00493-7>.
- [42] M.A. Darwish, T.I. Zubar, O.D. Kanafyev, D. Zhou, E.L. Trukhanova, S. V. Trukhanov, A.V. Trukhanov, A. Maher Henaiash, Combined effect of microstructure, surface energy, and adhesion force on the friction of PVA/ferrite spinel nanocomposites, *Mdp. Com.* 12 (2022), <https://doi.org/10.3390/nano121998>.
- [43] T.I. Zubar, V.M. Fedosyuk, S.V. Trukhanov, D.I. Tishkevich, D. Michels, D. Lyakhov, A.V. Trukhanov, Method of surface energy investigation by lateral AFM: application to control growth mechanism of nanostructured NiFe films, *Sci. Rep.* 10 (2020) 14411, <https://doi.org/10.1038/s41598-020-71416-w>.
- [44] A. Khaloo, M.H. Mobini, P. Hosseini, Influence of different types of nano-SiO₂ particles on properties of high-performance concrete, *Constr. Build. Mater.* 113 (2016) 188–201, <https://doi.org/10.1016/j.conbuildmat.2016.03.041>.
- [45] S.S. Ray, P.R.T. Peddinti, R. Soni, B. Kim, Y.I. Park, I.C. Kim, C.Y. Lee, Y.N. Kwon, Effectiveness of nanoparticles-based ultrahydrophobic coating for concrete materials, *J. Build. Eng.* 66 (2023), <https://doi.org/10.1016/j.jobe.2022.105799>.
- [46] L. Jiang, Z. Wang, X. Gao, M. Cui, Q. Yang, J. Qin, Effect of nanoparticles and surfactants on properties and microstructures of foam and foamed concrete, *Constr. Build. Mater.* 411 (2024), <https://doi.org/10.1016/j.conbuildmat.2023.134444>.
- [47] H.U. Ahmed, A.S. Mohammed, R.H. Faraj, A.A. Abdalla, S.M.A. Qadi, N.H. Sor, A.A. Mohammed, Innovative modeling techniques including MEP, ANN and FQ to forecast the compressive strength of geopolymer concrete modified with nanoparticles, *Neural Comput. Appl.* 35 (2023) 12453–12479, <https://doi.org/10.1007/s00521-023-08378-3>.
- [48] K. Kishore, A. Pandey, N.K. Wagri, A. Saxena, J. Patel, A. Al-Fakih, Technological challenges in nanoparticle-modified geopolymers concrete: A comprehensive review on nanomaterial dispersion, characterization techniques and its mechanical properties, *Case Stud. Constr. Mater.* 19 (2023), <https://doi.org/10.1016/j.cscm.2023.e02265>.
- [49] M.A. Othuman Mydin, P. Jagadessh, A. Bahrami, A. Dulaimi, Y.O. Özklıç, M.M. Al Bakri Abdullah, R.P. Jaya, Use of calcium carbonate nanoparticles in production of nano-engineered foamed concrete, *J. Mater. Res. Technol.* 26 (2023) 4405–4422, <https://doi.org/10.1016/j.jmrt.2023.08.106>.
- [50] G. Bunea, S.M. Alexa-Stratulat, P. Mihai, I.O. Toma, Use of Clay and Titanium Dioxide Nanoparticles in Mortar and Concrete—A State-of-the-Art Analysis, *Coatings* 13 (2023), <https://doi.org/10.3390/coatings13030506>.

- [51] G.F. Huseien, A Review on Concrete Composites Modified with Nanoparticles, *J. Compos. Sci.* 7 (2023), <https://doi.org/10.3390/jcs7020067>.
- [52] S. Ghorbanzadeh, M. Chamack, A.M. Mohammadi, N. Zoghi, Evaluation of the performance of concrete by adding silica nanoparticles and zeolite: a method deviation tolerance study, *Constr. Build. Mater.* 413 (2024), <https://doi.org/10.1016/j.conbuildmat.2024.134962>.
- [53] M. Zhang, L. Du, Z. Li, R. Xu, Durability of marine concrete doped with nanoparticles under joint action of Cl⁻ erosion and carbonation, *Case Stud. Constr. Mater.* 18 (2023), <https://doi.org/10.1016/j.cscm.2023.e01982>.
- [54] M. Mansourghanaei, M. Biklaryan, A. Mardookhpour, Experimental study of the effects of adding silica nanoparticles on the durability of geopolymmer concrete, *Aust. J. Civ. Eng.* 22 (2024) 81–93, <https://doi.org/10.1080/14488353.2022.2120247>.
- [55] K. Zhang, Q. Liu, H. Qian, B. Xiang, Q. Cui, J. Zhou, E. Chen, EATN: An Efficient Adaptive Transfer Network for Aspect-Level Sentiment Analysis, *IEEE Trans. Knowl. Data Eng.* 35 (2023) 377–389, <https://doi.org/10.1109/TKDE.2021.3075238>.
- [56] S. Kawashima, P. Hou, D.J. Corr, S.P. Shah, Modification of cement-based materials with nanoparticles, *Cem. Concr. Compos.* (2013) 8–15, <https://doi.org/10.1016/j.cemconcomp.2012.06.012>.
- [57] M.H. Zhang, J. Islam, Use of nano-silica to reduce setting time and increase early strength of concretes with high volumes of fly ash or slag, *Constr. Build. Mater.* 29 (2012) 573–580, <https://doi.org/10.1016/j.conbuildmat.2011.11.013>.
- [58] T. Meng, K. Ying, Y. Hong, Q. Xu, Effect of different particle sizes of nano-SiO₂ on the properties and microstructure of cement paste, *Nanotechnol. Rev.* 9 (2020) 833–842, <https://doi.org/10.1515/ntrev-2020-0066>.
- [59] M. Ramezani, Y.H. Kim, Z. Sun, Mechanical properties of carbon-nanotube-reinforced cementitious materials: database and statistical analysis, *Mag. Concr. Res.* 72 (2020) 1047–1071, <https://doi.org/10.1680/jmacr.19.00093>.
- [60] K. Narasimman, T.M. Jassam, T.S. Velayutham, M.M.M. Yaseer, R. Ruzaaimah, The synergic influence of carbon nanotube and nanosilica on the compressive strength of lightweight concrete, *J. Build. Eng.* 32 (2020), <https://doi.org/10.1016/j.jobe.2020.101719>.
- [61] C. Gunasekara, M. Sandanayake, Z. Zhou, D.W. Law, S. Setunge, Effect of nano-silica addition into high volume fly ash-hydrated lime blended concrete, *Constr. Build. Mater.* 253 (2020), <https://doi.org/10.1016/j.conbuildmat.2020.119205>.
- [62] M. Nili, A. Ehsani, Investigating the effect of the cement paste and transition zone on strength development of concrete containing nanosilica and silica fume, *Mater. Des.* 75 (2015) 174–183, <https://doi.org/10.1016/j.matdes.2015.03.024>.
- [63] M. Oltulu, R. Şahin, Effect of nano-SiO₂, nano-Al₂O₃ and nano-Fe₂O₃ powders on compressive strengths and capillary water absorption of cement mortar containing fly ash: A comparative study, *Energy Build.* 58 (2013) 292–301, <https://doi.org/10.1016/j.enbuild.2012.12.014>.
- [64] P. Zhang, J. Su, J. Guo, S. Hu, Influence of carbon nanotube on properties of concrete: a review, *Constr. Build. Mater.* 369 (2023) 130388, <https://doi.org/10.1016/j.conbuildmat.2023.130388>.
- [65] C. Zhuang, Y. Chen, The effect of nano-SiO₂ on concrete properties: a review, *Nanotechnol. Rev.* 8 (2019) 562–572, <https://doi.org/10.1515/ntrev-2019-0050>.
- [66] G. Bunea, S.M. Alexa-Stratulat, P. Mihaï, I.O. Toma, Use of clay and titanium dioxide nanoparticles in mortar and concrete—a state-of-the-art analysis, *Coatings* 13 (2023) 506, <https://doi.org/10.3390/coatings13030506>.
- [67] C. Belebchouche, S.E. Bensebti, C. Ould-Said, K. Moussaceb, S. Czarnecki, L. Sadowski, Stabilization of Chromium Waste by Solidification into Cement Composites, *Materials* 16 (2023) 6295, <https://doi.org/10.3390/ma16186295>.
- [68] E. Ghafari, S.A. Ghahari, Y. Feng, F. Severgnini, N. Lu, Effect of Zinc oxide and Al-Zinc oxide nanoparticles on the rheological properties of cement paste, *Compos. Part B Eng.* 105 (2016) 160–166, <https://doi.org/10.1016/j.compositesb.2016.08.040>.
- [69] Y. Zarea, S. Parhooodeh, L. Shahryari, A. Karbakhsh, Effect of zirconium oxide nanofiber on the strength and chloride ion penetration coefficient of concrete, *SN Appl. Sci.* 5 (2023) 1–9, <https://doi.org/10.1007/s42452-023-05471-z>.
- [70] O.A. Mohamed, M.M. Hazem, A. Mohsen, M. Ramadan, Impact of microporous γ-Al₂O₃ on the thermal stability of pre-cast cementitious composite containing glass waste, *Constr. Build. Mater.* 378 (2023) 131186, <https://doi.org/10.1016/j.conbuildmat.2023.131186>.
- [71] R.J.A. Sldozian, A.J. Hamad, H.S. Al-Rawis, Mechanical properties of lightweight green concrete including nano calcium carbonate, *J. Build. Pathol. Rehabil.* 8 (2023) 1–12, <https://doi.org/10.1007/s41024-022-00247-1>.
- [72] M. Wasim, T.D. Ngo, D. Law, A state-of-the-art review on the durability of geopolymers concrete for sustainable structures and infrastructure, Elsevier (2021), <https://doi.org/10.1016/j.conbuildmat.2021.123381>.
- [73] J. Xiao, C. Wang, T. Ding, A. Akbarnezhad, A recycled aggregate concrete high-rise building: structural performance and embodied carbon footprint, *J. Clean. Prod.* 199 (2018) 868–881, <https://doi.org/10.1016/j.jclepro.2018.07.210>.
- [74] A.M. Aly, M.S. El-Feky, M. Kohail, E.S.A.R. Nasr, Performance of geopolymers concrete containing recycled rubber, *Constr. Build. Mater.* 207 (2019) 136–144, <https://doi.org/10.1016/j.conbuildmat.2019.02.121>.
- [75] F.E. Jalal, M. Iqbal, W.A. Khan, A. Jamal, K. Onyelowie, Lekhraj, ANN-based swarm intelligence for predicting expansive soil swell pressure and compression strength, *Sci. Rep.* 14 (2024), <https://doi.org/10.1038/s41598-024-65547-7>.
- [76] H. Song, A. Ahmad, F. Farooq, K.A. Ostrowski, M. Maślak, S. Czarnecki, F. Aslam, Predicting the compressive strength of concrete with fly ash admixture using machine learning algorithms, *Constr. Build. Mater.* 308 (2021) 125021, <https://doi.org/10.1016/j.conbuildmat.2021.125021>.
- [77] C. Zhu, An adaptive agent decision model based on deep reinforcement learning and autonomous learning, *J. Logist. Inform. Serv. Sci.* 10 (2023) 107–118, <https://doi.org/10.33168/JLISS.2023.0309>.
- [78] U. Asif, M.F. Javed, M. Abuussain, M. Ali, W.A. Khan, A. Mohamed, Predicting the mechanical properties of plastic concrete: an optimization method by using genetic programming and ensemble learners, *Case Stud. Constr. Mater.* 20 (2024) e03135, <https://doi.org/10.1016/j.cscm.2024.e03135>.
- [79] A. Nafees, M.F. Javed, S. Khan, K. Nazir, F. Farooq, F. Aslam, M.A. Musarat, N. I. Vatin, Predictive modeling of mechanical properties of silica fume-based green concrete using artificial intelligence approaches: MLPNN, ANFIS, and GEP, *Materials* 14 (2021) 7531, <https://doi.org/10.3390/ma14247531>.
- [80] A. Ahmad, F. Farooq, P. Niewiadomski, K. Ostrowski, A. Akbar, F. Aslam, R. Alyousef, Prediction of compressive strength of fly ash based concrete using individual and ensemble algorithm, *Materials* 14 (2021) 1–21, <https://doi.org/10.3390/ma14040794>.
- [81] C. Madubuchukwu Nwakaire, S. Poh Yap, C. Chuen Onn, C. Wah Yuen, H. Adebayo Ibrahim, Utilisation of recycled concrete aggregates for sustainable highway pavement applications; a review, *Constr. Build. Mater.* 235 (2020), <https://doi.org/10.1016/j.conbuildmat.2019.117444>.
- [82] X. Chang, J. Guo, H. Qin, J. Huang, X. Wang, P. Ren, Single-objective and multi-objective flood interval forecasting considering interval fitting coefficients, *Water Resour. Manag.* (2024), <https://doi.org/10.1007/s11269-024-03848-2>.
- [83] X. Jiang, Y. Wang, D. Zhao, L. Shi, Online Pareto optimal control of mean-field stochastic multi-player systems using policy iteration, *Sci. China Inf. Sci.* 67 (2024), <https://doi.org/10.1007/s11432-023-3982-y>.
- [84] H.S. Ullah, R.A. Khushnood, F. Farooq, J. Ahmad, N.I. Vatin, D.Y.Z. Ewais, Prediction of Compressive Strength of Sustainable Foam Concrete Using Individual and Ensemble Machine Learning Approaches, *Materials (Basel)* 15 (2022), <https://doi.org/10.3390/ma15093166>.
- [85] A. Ahmad, F. Farooq, K.A. Ostrowski, K. Śliwa-Wieczorek, S. Czarnecki, Application of novel machine learning techniques for predicting the surface chloride concentration in concrete containing waste material, *Materials* 14 (2021) 2297, <https://doi.org/10.3390/ma14092297>.
- [86] M.F. Javed, F. Farooq, S.A. Memon, A. Akbar, M.A. Khan, F. Aslam, R. Alyousef, H. Alabduljabbar, S.K. Ur Rehman, New prediction model for the ultimate axial capacity of concrete-filled steel tubes: an evolutionary approach, *Crystals* 10 (2020) 1–33, <https://doi.org/10.3390/cryst10090741>.
- [87] N.S. Alghrairi, F.N. Aziz, S.A. Rashid, M.Z. Mohamed, M. Ibrahim, Machine learning-based compressive strength estimation in nanomaterial-modified lightweight concrete, *Open Eng.* 14 (2024), <https://doi.org/10.1515/eng-2022-0604>.
- [88] M. Kioumarsi, H. Dabiri, A. Kandiri, V. Farhangi, Compressive strength of concrete containing furnace blast slag: optimized machine learning-based models, *Clean. Eng. Technol.* 13 (2023) 100604, <https://doi.org/10.1016/j.clet.2023.100604>.
- [89] H. Jiao, Y. Wang, L. Li, K. Arif, F. Farooq, A. Alaskar, A novel approach in forecasting compressive strength of concrete with carbon nanotubes as nanomaterials, *Mater. Today Commun.* 35 (2023) 106335, <https://doi.org/10.1016/j.mtcomm.2023.106335>.
- [90] H.P. Zhang, X.C. Li, M.N. Amin, A.A. Alawi Al-Naghhi, S.U. Arifeen, F. Althoeey, A. Ahmad, Analyzing chloride diffusion for durability predictions of concrete using contemporary machine learning strategies, *Mater. Today Commun.* 38 (2024) 108543, <https://doi.org/10.1016/j.mtcomm.2024.108543>.
- [91] F. Farooq, W. Ahmed, A. Akbar, F. Aslam, R. Alyousef, Predictive modeling for sustainable high-performance concrete from industrial wastes: a comparison and optimization of models using ensemble learners, *J. Clean. Prod.* 292 (2021), <https://doi.org/10.1016/j.jclepro.2021.126032>.
- [92] J. Yang, P.L. Yee, A.A. Khan, H. Karamiti, E.T. Eldin, A. Aldweesh, A. El Jery, L. Hussain, A. Omar, Intelligent lung cancer MRI prediction analysis based on cluster prominence and posterior probabilities utilizing intelligent Bayesian methods on extracted gray-level co-occurrence (GLCM) features, *Digit. Heal.* 9 (2023), <https://doi.org/10.1177/20552076231172632>.
- [93] H. Moayedi, A. Mosavi, A water cycle-based error minimization technique in predicting the bearing capacity of shallow foundation, *Eng. Comput.* 38 (2022) 3993–4006, <https://doi.org/10.1007/s00366-021-01289-8>.
- [94] P.G. Asteria, P.B. Lourenço, P.C. Roussis, C. Elpida Adami, D.J. Armaghani, L. Cavalieri, C.E. Chalioris, M. Hajihassani, M.E. Lemonis, A.S. Mohammed, K. Pilakoutas, Revealing the nature of metakaolin-based concrete materials using artificial intelligence techniques, *Constr. Build. Mater.* 322 (2022), <https://doi.org/10.1016/j.conbuildmat.2022.126500>.
- [95] M. Ehteram, F. Panahi, A.N. Ahmed, A.H. Mosavi, A. El-Shafie, Inclusive multiple model using hybrid artificial neural networks for predicting evaporation, *Front. Environ. Sci.* 9 (2022) 652, <https://doi.org/10.3389/fenvs.2021.789995>.
- [96] M. Raheel, M. Iqbal, R. Khan, M. Alam, M. Azab, S.M. Eldin, Application of gene expression programming to predict the compressive strength of quaternary-blended concrete, *Asian J. Civ. Eng.* 24 (2023) 1351–1364, <https://doi.org/10.1007/s42107-023-00573-w>.
- [97] S. Shi, D. Han, M. Cui, A multimodal hybrid parallel network intrusion detection model, *Conn. Sci.* 35 (2023) 2227780, <https://doi.org/10.1080/09540091.2023.2227780>.
- [98] A.D. Shakibjoo, M. Moradzadeh, S.U. Din, A. Mohammadzadeh, A.H. Mosavi, L. Vandeveld, Optimized type-2 fuzzy frequency control for multi-area power systems, *IEEE Access* 10 (2022) 6989–7002, <https://doi.org/10.1109/ACCESS.2021.3139259>.
- [99] W. Zheng, A. Zaman, F. Farooq, F. Althoeey, A. Alaskar, A. Akbar, Sustainable predictive model of concrete utilizing waste ingredient: individual algorithms

- with optimized ensemble approaches, *Mater. Today Commun.* 35 (2023) 105901, <https://doi.org/10.1016/j.mtcomm.2023.105901>.
- [100] M.F. Javed, F. Farooq, S.A. Memon, A. Akbar, M.A. Khan, F. Aslam, R. Alyousef, H. Alabduljabbar, S.K.U. Rehman, New prediction model for the ultimate axial capacity of concrete-filled steel tubes: an evolutionary approach, *Crystals* 10 (2020) 741, <https://doi.org/10.3390/cryst10090741>.
- [101] M.A. Khan, A. Zafar, F. Farooq, M.F. Javed, R. Alyousef, H. Alabduljabbar, M. I. Khan, Geopolymer concrete compressive strength via artificial neural network, adaptive fuzzy interface system, and gene expression programming With K-fold cross validation, *Front. Mater.* 8 (2021), <https://doi.org/10.3389/fmats.2021.621163>.
- [102] H. Wang, D. Han, M. Cui, C. Chen, NAS-YOLOX: a SAR ship detection using neural architecture search and multi-scale attention, *Conn. Sci.* 35 (2023) 1–32, <https://doi.org/10.1080/09540091.2023.2257399>.
- [103] D.K. Thai, T.M. Tu, T.Q. Bui, T.T. Bui, Gradient tree boosting machine learning on predicting the failure modes of the RC panels under impact loads, *Eng. Comput.* 3 (1) (2019), <https://doi.org/10.1007/s00366-019-00842-w>.
- [104] M. Liang, Z. Chang, Z. Wan, Y. Gan, E. Schlangen, B. Šavija, Interpretable Ensemble-Machine-Learning models for predicting creep behavior of concrete, *Cem. Concr. Compos.* 125 (2022) 104295, <https://doi.org/10.1016/j.cemconcomp.2021.104295>.
- [105] Q.H. Tran, H. Nguyen, X.N. Bui, Novel Soft Computing Model for Predicting Blast-Induced Ground Vibration in Open-Pit Mines Based on the Bagging and Sibling of Extra Trees Models, *C. - Comput. Model. Eng. Sci.* 134 (2023) 2227–2246, <https://doi.org/10.32604/cmes.2022.021893>.
- [106] Y. Parasher, G. Kaur, P. Tomar, A. Kaushik, Development of artificial neural network to predict the concrete strength, in: *Smart Innov. Syst. Technol.*, Springer, 2020, pp. 379–389, https://doi.org/10.1007/978-981-13-8406-6_36.
- [107] D. Han, H.X. Zhou, T.H. Weng, Z. Wu, B. Han, K.C. Li, A.S.K. Pathan, LMCA: a lightweight anomaly network traffic detection model integrating adjusted mobilenet and coordinate attention mechanism for IoT, *Telecommun. Syst.* 84 (2023) 549–564, <https://doi.org/10.1007/S11235-023-01059-5>.
- [108] J. Sun, Y. Ma, J. Li, J. Zhang, Z. Ren, X. Wang, Machine learning-aided design and prediction of cementitious composites containing graphite and slag powder, *J. Build. Eng.* 43 (2021) 102544, <https://doi.org/10.1016/j.jobe.2021.102544>.
- [109] D.L. Chen, J.W. Zhao, S.R. Qin, SVM strategy and analysis of a three-phase quasi-Z-source inverter with high voltage transmission ratio, *Sci. China Technol. Sci.* 66 (2023) 2996–3010, <https://doi.org/10.1007/S11431-022-2394-4>.
- [110] X. Yuan, Y. Tian, W. Ahmad, A. Ahmad, K.I. Usanova, A.M. Mohamed, R. Khallaf, Machine learning prediction models to evaluate the strength of recycled aggregate concrete, *Materials* 15 (2022), <https://doi.org/10.3390/mma15082823>.
- [111] A. Nafees, M.N. Amin, K. Khan, K. Nazir, M. Ali, M.F. Javed, F. Aslam, M. A. Musarat, N.I. Vatin, Modeling of mechanical properties of silica fume-based green concrete using machine learning techniques, *Polymers* 14 (2022) 30, <https://doi.org/10.3390/polym14010030>.
- [112] J. Zhang, D. Li, Y. Wang, Toward intelligent construction: Prediction of mechanical properties of manufactured-sand concrete using tree-based models, *J. Clean. Prod.* 258 (2020) 120665, <https://doi.org/10.1016/j.jclepro.2020.120665>.
- [113] L. Qiao, P. Miao, G. Xing, X. Luo, J. Ma, M.A. Farooq, Interpretable machine learning model for predicting freeze-thaw damage of dune sand and fiber reinforced concrete, *Case Stud. Constr. Mater.* 19 (2023), <https://doi.org/10.1016/j.cscm.2023.e02453>.
- [114] V. Quan Tran, Machine learning approach for investigating chloride diffusion coefficient of concrete containing supplementary cementitious materials, *Constr. Build. Mater.* 328 (2022), <https://doi.org/10.1016/j.conbuildmat.2022.127103>.
- [115] T.G. Wakjira, M. Ibrahim, U. Ebead, M.S. Alam, Explainable machine learning model and reliability analysis for flexural capacity prediction of RC beams strengthened in flexure with FRCM, *Eng. Struct.* 255 (2022), <https://doi.org/10.1016/j.engstruct.2022.113903>.
- [116] P. Thisovithan, H. Aththanayake, D.P.P. Meddage, I.U. Ekanayake, U. Rathnayake, A novel explainable AI-based approach to estimate the natural period of vibration of masonry infill reinforced concrete frame structures using different machine learning techniques, *Results Eng.* 19 (2023) 101388, <https://doi.org/10.1016/j.RINENG.2023.101388>.
- [117] F. Aslam, M. Zubair, Supplementary cementitious materials in blended cement concrete: Advancements in predicting compressive strength through machine learning, *Mater. Today Commun.* 38 (2024) 107725, <https://doi.org/10.1016/j.mtcomm.2023.107725>.
- [118] S. Ul Arifeen, M. Nasir Amin, W. Ahmad, F. Althoey, M. Ali, B. Saad Alotaibi, M. Awad Abuhussain, A comparative study of prediction models for alkali-activated materials to promote quick and economical adaptability in the building sector, *Constr. Build. Mater.* 407 (2023), <https://doi.org/10.1016/j.conbuildmat.2023.133485>.
- [119] S.I. Malami, A.A. Musa, S.I. Haruna, U.U. Aliyu, A.G. Usman, M.I. Abdurrahman, A. Bashir, S.I. Abba, Implementation of soft-computing models for prediction of flexural strength of pervious concrete hybridized with rice husk ash and calcium carbide waste, *Model. Earth Syst. Environ.* 8 (2022) 1933–1947, <https://doi.org/10.1007/s40808-021-01195-4>.
- [120] J. Dou, J. Liu, Y. Wang, L. Zhi, J. Shen, G. Wang, Surface activity, wetting, and aggregation of a perfluoropolyether quaternary ammonium salt surfactant with a hydroxyethyl group, *Molecules* 28 (2023), <https://doi.org/10.3390/molecules28207151>.
- [121] R. Fei, Y. Guo, J. Li, B. Hu, L. Yang, An improved BPNN method based on probability density for indoor location, *IEICE Trans. Inf. Syst.* E106.D (2023) 773–785, <https://doi.org/10.1587/transinf.2022DLP0073>.
- [122] J.H. Friedman, Greedy function approximation: a gradient boosting machine, *Ann. Stat.* 29 (2001) 1189–1232, <https://doi.org/10.1214/aos/1013203451>.
- [123] M.W. Ahmad, M. Mourshed, Y. Rezgui, Trees vs Neurons: Comparison between random forest and ANN for high-resolution prediction of building energy consumption, *Energy Build.* 147 (2017) 77–89, <https://doi.org/10.1016/j.enbuild.2017.04.038>.
- [124] Y. Zhao, J. Wang, G. Cao, Y. Yuan, X. Yao, L. Qi, Intelligent control of multilegged robot smooth motion: a review, *IEEE Access* 11 (2023) 86645–86685, <https://doi.org/10.1109/ACCESS.2023.3304992>.
- [125] S. Meng, F. Meng, H. Chi, H. Chen, A. Pang, A robust observer based on the nonlinear descriptor systems application to estimate the state of charge of lithium-ion batteries, *J. Franklin Inst.* 360 (2023) 11397–11413, <https://doi.org/10.1016/j.jfranklin.2023.08.037>.
- [126] L. Sun, M. Koopialipoor, D. Jahed Armaghani, R. Tarinejad, M.M. Tahir, Applying a meta-heuristic algorithm to predict and optimize compressive strength of concrete samples, *Eng. Comput.* 37 (2021) 1133–1145, <https://doi.org/10.1007/s00366-019-00875-1>.
- [127] J. Li, H. Tang, X. Li, H. Dou, R. Li, LEF-YOLO: a lightweight method for intelligent detection of four extreme wildfires based on the YOLO framework, *Int. J. Wildl. Fire* 33 (2023), <https://doi.org/10.1071/WF23044>.
- [128] J. Guo, Y. Liu, Q. Zou, L. Ye, S. Zhu, H. Zhang, Study on optimization and combination strategy of multiple daily runoff prediction models coupled with physical mechanism and LSTM, *J. Hydrol.* 624 (2023), <https://doi.org/10.1016/j.jhydrol.2023.129969>.
- [129] W. Liang, S. Luo, G. Zhao, H. Wu, Predicting hard rock pillar stability using GBBDT, XGBoost, and LightGBM algorithms, *Mathematics* 8 (2020), <https://doi.org/10.3390/MATH8050765>.
- [130] H. Zeng, C. Yang, H. Zhang, Z. Wu, J. Zhang, G. Dai, F. Babiloni, W. Kong, L. Chuang, A lightgbm-based eeg analysis method for driver mental states classification, *Comput. Intell. Neurosci.* 2019 (2019), <https://doi.org/10.1155/2019/3761203>.
- [131] C. Zhu, X. Li, C. Wang, B. Zhang, B. Li, Deep learning-based coseismic deformation estimation from insar interferograms, *IEEE Trans. Geosci. Remote Sens.* 62 (2024) 1–10, <https://doi.org/10.1109/TGRS.2024.3357190>.
- [132] J. Xin, W. Xu, B. Cao, T. Wang, S. Zhang, A deep-learning-based MAC for integrating channel access, rate adaptation and channel switch, (2024). ([http://arxiv.org/abs/2406.02291](https://arxiv.org/abs/2406.02291)) (accessed July 13, 2024).
- [133] H. Kodaz, S. Özçen, A. Arslan, S. Güneş, Medical application of information gain based artificial immune recognition system (AIRS): diagnosis of thyroid disease, *Expert Syst. Appl.* 36 (2009) 3086–3092, <https://doi.org/10.1016/j.eswa.2008.01.026>.
- [134] D. Ghunimat, A.E. Alzoubi, A. Alzboon, S. Hanandeh, Prediction of concrete compressive strength with GGBFS and fly ash using multilayer perceptron algorithm, random forest regression and k-nearest neighbor regression, *Asian J. Civ. Eng.* 24 (2023) 169–177, <https://doi.org/10.1007/s42107-022-00495-z>.
- [135] H. Franco-Lopez, A.R. Ek, M.E. Bauer, Estimation and mapping of forest stand density, volume, and cover type using the k-nearest neighbors method, *Remote Sens. Environ.* 77 (2001) 251–274, [https://doi.org/10.1016/S0034-4257\(01\)00209-7](https://doi.org/10.1016/S0034-4257(01)00209-7).
- [136] A. Mohammed, L. Burhan, K. Ghafor, W. Sarwar, W. Mahmood, Artificial neural network (ANN), M5P-tree, and regression analyses to predict the early age compression strength of concrete modified with DBC-21 and VK-98 polymers, *Neural Comput. Appl.* 33 (2021) 7851–7873, <https://doi.org/10.1007/s00521-020-05525-y>.
- [137] H.U. Ahmed, A.A.S.A.A. Mohammed, R.H. Faraj, A.A. Abdalla, S.M.A. Qaidi, N. H. Sor, A.A.S.A.A. Mohammed, Innovative modeling techniques including MEP, ANN and FQ to forecast the compressive strength of geopolymer concrete modified with nanoparticles, *Neural Comput. Appl.* 35 (2023) 1–27, <https://doi.org/10.1007/s00521-023-08378-3>.
- [138] A. Beycioğlu, M. Emiroğlu, Y. Kocak, S. Subaşı, Analyzing the compressive strength of clinker mortars using approximate reasoning approaches - ANN vs MLR, *Comput. Concr.* 15 (2015) 89–101, <https://doi.org/10.12989/cac.2015.15.1.089>.
- [139] S.S. Rizvon, K. Jayakumar, Strength prediction models for recycled aggregate concrete using Random Forests, ANN and LASSO, *J. Build. Pathol. Rehabil.* 7 (2022), <https://doi.org/10.1007/s41024-021-00145-y>.
- [140] D. Nagarajan, T. Rajagopal, N. Meyappan, A comparative study on prediction models for strength properties of lwa concrete using artificial neural network, *Rev. La Constr.* 19 (2020), <https://doi.org/10.7764/RDLC.19.1.103-111>.
- [141] H.U. Ahmed, A.S. Mohammed, R.H. Faraj, A.A. Abdalla, S.M.A. Qaidi, N.H. Sor, A.A. Mohammed, Innovative modeling techniques including MEP, ANN and FQ to forecast the compressive strength of geopolymer concrete modified with nanoparticles, *Neural Comput. Appl.* 35 (2023) 12453–12479, <https://doi.org/10.1007/s00521-023-08378-3>.
- [142] T.D. Nguyen, T.H. Tran, N.D. Hoang, Prediction of interface yield stress and plastic viscosity of fresh concrete using a hybrid machine learning approach, *Adv. Eng. Inform.* 44 (2020) 101057, <https://doi.org/10.1016/j.aei.2020.101057>.
- [143] G. Xu, G. Zhou, F. Althoey, H.M. Hadidi, A. Alaskar, A.M. Hassan, F. Farooq, Evaluation of properties of bio-composite with interpretable machine learning approaches: optimization and hyper tuning, *J. Mater. Res. Technol.* 25 (2023) 1421–1446, <https://doi.org/10.1016/j.jmrt.2023.06.007>.
- [144] W. Dong, Y. Huang, B. Lehane, G. Ma, Multi-objective design optimization for graphite-based nanomaterials reinforced cementitious composites: a data-driven method with machine learning and NSGA-II, *Constr. Build. Mater.* 331 (2022) 127198, <https://doi.org/10.1016/j.conbuildmat.2022.127198>.
- [145] M.F. Iqbal, M.F. Javed, M. Rauf, I. Azim, M. Ashraf, J. Yang, Q. Feng Liu, Sustainable utilization of foundry waste: forecasting mechanical properties of

- foundry sand based concrete using multi-expression programming, *Sci. Total Environ.* 780 (2021) 146524, <https://doi.org/10.1016/j.scitotenv.2021.146524>.
- [146] D.N. Moriasi, J.G. Arnold, M.W. Van Liew, R.L. Bingner, R.D. Harmel, T.L. Veith, Model evaluation guidelines for systematic quantification of accuracy in watershed simulations, *Trans. ASABE* 50 (2007) 885–900. (<https://elibrary.asabe.org/abstract.asp?aid=23153>). accessed October 9, 2023.
- [147] A. Ahmed, W. Song, Y. Zhang, M.A. Haque, X. Liu, Hybrid BO-XGBoost and BO-RF models for the strength prediction of self-compacting mortars with parametric analysis, *Materials* 16 (2023), <https://doi.org/10.3390/ma16124366>.
- [148] T. Chen, C. Guestrin, XGBoost: a scalable tree boosting system, in: : Proc. ACM SIGKDD Int. Conf. Knowl. Discov. Data Min. (2016) 785–794, <https://doi.org/10.1145/2939672.2939785>.
- [149] G. Ke, Q. Meng, T. Finley, T. Wang, W. Chen, W. Ma, Q. Ye, T.Y. Liu, LightGBM: a highly efficient gradient boosting decision tree, *Adv. Neural Inf. Process. Syst.* (2017) 3147–3155, in: (<https://proceedings.neurips.cc/paper/2017/hash/6449f44a102fde848669bdd9eb6b76fa-Abstract.html>). accessed June 24, 2024.
- [150] A.T. Amlashi, P. Alidoust, A.R. Ghanizadeh, S. Khabiri, M. Pazhouhi, M. S. Monabati, Application of computational intelligence and statistical approaches for auto-estimating the compressive strength of plastic concrete, *Eur. J. Environ. Civ. Eng.* 26 (2022) 3459–3490, <https://doi.org/10.1080/19648189.2020.1803144>.